九州大学学術情報リポジトリ
Kyushu University Institutional Repository

SPECTROSCOPIC STUDIES ON COMPLEXATION EQUILIBRIA IN THE CROSS-LINKED POLYMER SOLUTION

宮崎, 義信
九州大学理学研究科化学専攻

https://doi.org/10.11501/3065452

出版情報：九州大学, 1992, 博士（理学）, 課程博士
バージョン：
権利関係：

KYUSHU UNIVERSITY

SPECTROSCOPIC STUDIES ON COMPLEXATION EQUILIBRIA IN THE CROSS-LINKED POLYMER SOLUTION

宮崎義信

(1)

SPECTROSCOPIC STUDIES ON COMPLEXATION EQUILIBRIA IN THE CROSS-LINKED POLYMER SOLUTION

YOSHINOBU MIYAZAKI

CONTENTS

		Page
PREFACE		1
CHAPTER 1.	ABSORPTION SPECTROSCOPIC STUDIES ON COMPLEXATION EQUILIBRIA OF INORGANIC COBALT(II) COMPLEXES IN ION-EXCHANGERS	2
CHAPTER 2.	^{31}P NMR SPECTROSCOPIC STUDIES ON COMPLEXATION EQUILIBRIA OF CADMIUM(II)-PHOSPHINATE COMPLEXES IN CATION-EXCHANGERS	25
CHAPTER 3.	^{11}B NMR SPECTROSCOPIC STUDIES ON COMPLEXATION EQUILIBRIA OF BORATE-DIHYDROXYCARBOXYLATE COMPLEXES IN ANION-EXCHANGE RESINS	44
CHAPTER 4.	^{31}P AND ^{13}C NMR SPECTROSCOPIC STUDIES ON PROTONATION EQUILIBRIA OF OXOANIONS IN CROSS-LINKED DEXTRAN GELS	53
CHAPTER 5.	^{27}Al NMR SPECTROSCOPIC STUDIES ON COMPLEXATION EQUILIBRIA OF ALUMINIUM ION IN CROSS-LINKED DEXTRAN GELS	73
CONCLUSIONS		83
REFERENCES		86
ACKNOWLEDGMENTS		89

PREFACE

A biological medium is thought to be an aqueous solution of multicomponent system which contains low molecular-weight organic and inorganic electrolytes, non-charged organic compounds, polymers and polyelectrolytes. Various types of biochemical reactions, such as complex formation and oxidation-reduction reactions occur in such colloidal solutions. Polyelectrolytes, such as nucleic acids and proteins, constitute the matrix that contains fixed charge ion-exchange sites (e.g. phosphate and carboxylate). In this point, a cross-linked polymer gel, in particular an ion-exchanger, can be a model for the biological medium. Moreover, ion-exchangers are widely used for practical purposes in industry and analytical chemistry. To study complexation equilibria in the gel internal solution is very useful for understanding the chemical reaction in the biological system as well as for practical purposes.

In this study, direct spectroscopic methods such as electronic and NMR spectroscopies were successfully employed to the analysis of complexation equilibria in the cross-linked polymer gel phase. For example, visible absorption spectra of inorganic cobalt(II) complexes within cation- and anion-exchangers were observed and stability constants of the complex were determined by the spectral analyses. NMR spectra (^{31}P, ^{13}C, ^{11}B and ^{27}Al) of species within the gel were observed and the characteristic NMR properties were discussed. The stability constants were also determined by the NMR methods. The complexibility in the gel phase was compared with that in an ordinary solution and the difference in complexibility between these phases was discussed in detail.

CHAPTER 1. ABSORPTION SPECTROSCOPIC STUDIES ON COMPLEXATION EQUILIBRIA OF INORGANIC COBALT(II) COMPLEXES IN ION-EXCHANGERS

INTRODUCTION

Although a large number of studies on complex formation in solutions using an ion-exchange method have so far been reported,[1-4] little has been noted on the complex formation within the ion-exchanger phase itself. It is only known that the very high complexation of metal ions in the anion-exchanger phase is due to the high ligand anion concentration and that the very low complexation in the cation-exchanger phase due to the exclusion of ligand anions. It was considered, however, that there should also be other factors such as dielectric constant, spatial restriction and internal pressure influencing complexation in the ion-exchanger phase.

In this chapter, absorption spectroscopic studies on the formation of cobalt(II) complexes with inorganic ligands, such as chloride and thiocyanate, in ion-exchanger solid phases will be treated. An intrinsic difference in complexation between the ion-exchanger phase and an ordinary solution phase will also be described in detail.

EXPERIMENTAL

Apparatus, reagents and ion-exchangers

A Hitachi recording spectrophotometer EPS-3T was employed for absorbance measurements. All reagents used were of commercially available reagent grade. Deionized and distilled water was used thoroughout. Cation-exchangers of different cross-linking degrees, Dowex 50W-X2, -X4 and -X8 (100 - 200 mesh) of the sodium form; and a cross-linked dextran gel-type cation-exchanger, SP-Sephadex C-25 (Pharmacia, Uppsala, Sweden) of the sodium form; were used in determining the stability constant of the one-to-one cobalt(II)-isothiocyanate complex in each ion-exchanger phase.

Measurement and analysis of absorption spectra

A technique for the absorbance measurements of an ion-exchanger layer and its quantitative treatment have already been developed.[5-7] The ion-exchanger beads in which the complexes had been sorbed were packed into a 2 mm quartz cell with a small amount of equilibrated solution, and the absorption spectrum was recorded using a Hitachi recording spectrophotometer EPS-3T. A net absorption spectrum on the sorbed chemical components was obtained by subtracting the absorbance of the interstitial solution from the observed overall absorbance of the sample layer. In order to make a correct spectral analysis, the net light path length of the ion-exchanger solid phase in the cell, as well as that of the interstitial solution, must be known. They were experimentally determined separately as follows.

A potassium hexacyanoferrate(III) solution was used to determine the light path length of the interstitial solution. Since highly-charged anions such as $Fe(CN)_6^{3-}$ are almost entirely excluded from the cation-exchanger phase, the visible absorption spectrum of the cation-exchanger layer containing a potassium hexacyanoferrate(III) solution should be ascribed to that of the interstitial solution. The net light path length of the interstitial solution in this cell can be obtained (in mm) by

$$l_i = 2\frac{A_i}{A_s} \qquad (1)$$

where A_s and A_i are the absorbances of the equilibrated solution (using a 2 mm cell) and of the cation-exchanger layer (for a 2 mm cell), respectively.

In obtaining the light path length of the cation-exchanger phase in the same cell, a praseodymium chloride solution was used. The molar absorptivity of the praseodymium cation may be almost constant irrespective of its solution environment, namely, the molar absorptivity of the metal ion in the cation-exchanger phase is considered to be the same as that in the solution. Thus, the light path length of the cation-exchanger phase (in mm) in the cell can be calculated by

$$l = \frac{\overline{A}^* - A_i}{\varepsilon_{Pr}\bar{C}_{Pr}} \qquad (2)$$

where $\overline{A}^*$ is the overall absorbance of the ion-exchanger layer, A_i the absorbance of the interstitial equilibrated solution calculated using eq. (1), ε_{Pr} the molar absorptivity of the praseodymium ion and $\bar{C}_{Pr}$ the praseodymium ion concentration in the cation-exchanger phase expressed in mol dm^{-3}.

Measurement of free thiocyanate ion concentration in cation-exchanger phase

Each of about five grams of cation-exchangers, Dowex 50W-X2, -X4 and -X8 (100 - 200 mesh) of the sodium form, and about one gram of SP-Sephadex C-25 of the sodium form, were equilibrated with 25 cm^3 of a solution ($I = 0.5$) containing sodium thiocyanate and sodium perchlorate solution by a column operation. After equilibrium, the volume of the cation-exchanger bed was measured. Then, the net volume of the cation-exchanger phase including the ion-exchanger skeleton was calculated from the bed volume, using the ratio of the volume of the interstitial space to the bed volume (0.37 for Dowex resins and 0.50 for SP-Sephadex C-25).[8] The interstitial solution in the cation-exchanger bed was stripped with water and the amount of the free thiocyanate ion in the bed was determined spectrophotometrically using ferric chloride. The free thiocyanate ion concentration in the cation-exchanger phase was obtained by subtracting the amount of the free thiocyanate ion in the interstitial equilibrated solution from that in the bed, expressed in the volume base (mol dm^{-3}).

RESULTS AND DISCUSSION

Light path parameters of the ion-exchanger particle layer

The absorption spectrum for the cation-exchanger layer of Dowex 50W-X4 (100 - 200 mesh) equilibrated with a solution containing 0.004 mol dm^{-3} potassium hexacyanoferrate(III) and 0.5 mol dm^{-3} hydrochloric acid is shown in Fig. 1. The light path length of the interstitial solution was found to be 0.755 mm for a 2 mm

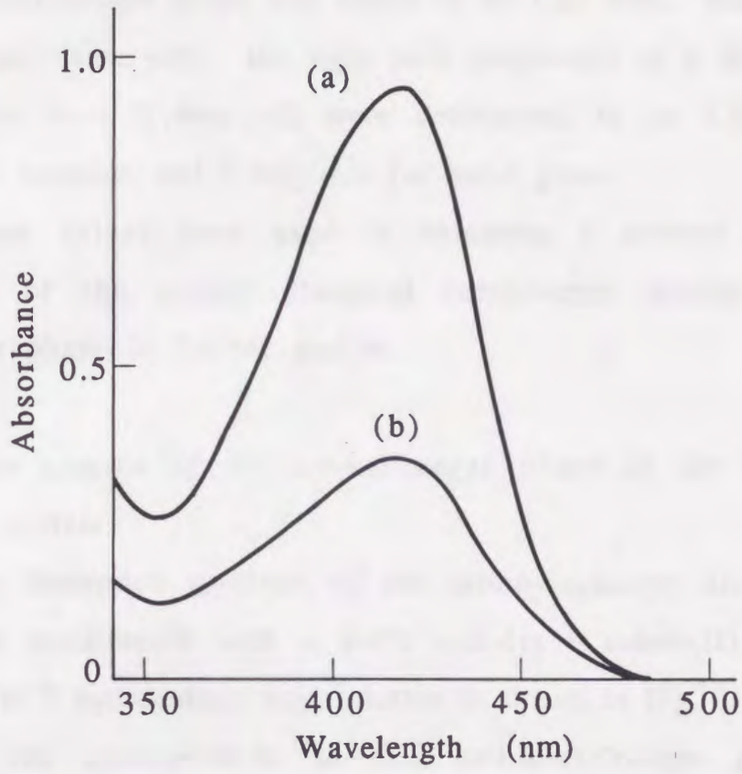

Fig. 1. Determination of the light path length for an interstitial solution with a 2 mm cell.

(a) The absorption spectrum for a Dowex 50W-X4 layer equilibrated with a 0.004 mol dm^{-3} $K_3Fe(CN)_6$ - 0.5 mol dm^{-3} HCl solution.

(b) The solution spectrum of the equilibrated solution.

cell using eq. (1), by comparison with the equilibrated solution spectrum. The absorption spectrum for the cation-exchanger phase of the same resin, equilibrated with a 0.05 mol dm^{-3} praseodymium chloride - 0.5 mol dm^{-3} perchloric acid solution using a 2 mm cell, is given in Fig. 2. The net light path length of the cation-exchanger phase was found to be 1.25 mm, using eq. (2).

In the same way, the light path parameters of a SP-Sephadex C-25 layer in a 2 mm cell were determined to be 1.02 mm for interstitial solution and 0.865 mm for solid phase.

These values were used in obtaining a correct absorption spectrum of the sorbed chemical components within the ion-exchanger phase in further studies.

Absorption spectra of the ion-exchanger phase in the cobalt(II)*-chloride system*

The absorption spectrum of the cation-exchanger Dowex 50W-X4 phase equilibrated with a 0.476 mol dm^{-3} cobalt(II) chloride - 5.4 mol dm^{-3} hydrochloric acid solution is shown in Fig. 3. The total chloride ion concentration in this cation-exchanger phase was calculated to be 2.64 mol dm^{-3} from the amount of chloride ions sorbed and the net volume of the ion-exchanger phase. For comparison, the absorption spectrum of a 0.290 mol dm^{-3} cobalt(II) chloride - 2.06 mol dm^{-3} hydrochloric acid solution which has the same total chloride concentration is shown in the figure. Furthermore, the spectrum of the anion-exchanger Muromac AG 1-X4 phase equilibrated with a 0.290 mol dm^{-3} cobalt(II) chloride-1.84 mol dm^{-3} hydrochloric acid solution is also shown, where the counter-chloride concentration in the anion-exchanger phase is again 2.64 mol dm^{-3}.

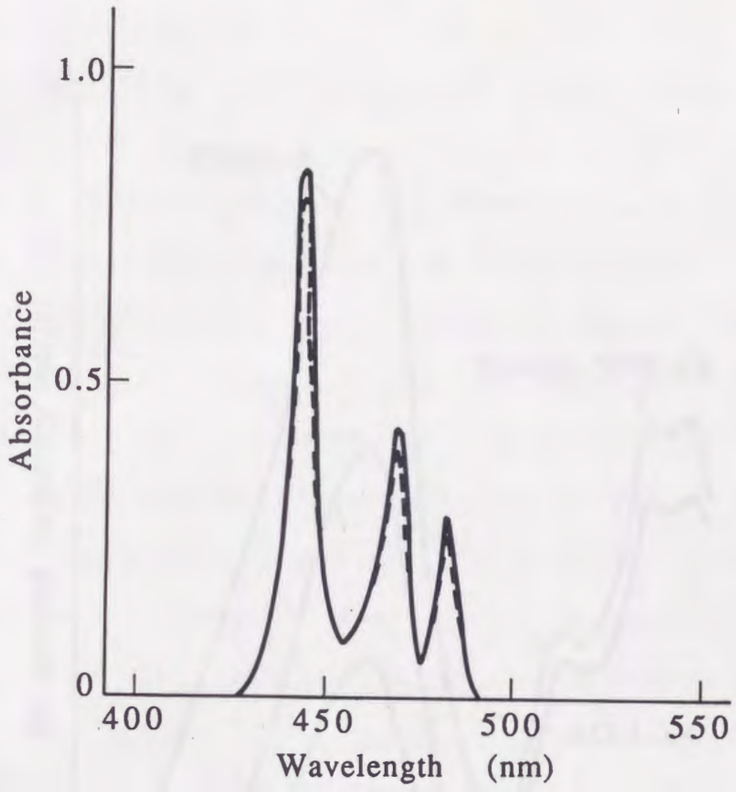

Fig. 2. Determination of the net absorbance by praseodymium in the ion-exchanger phase with a 2 mm cell.
Solid line : overall absorption spectrum for a Dowex 50W-X4 layer equilibrated with a 0.05 mol dm^{-3} $PrCl_3$ - 0.5 mol dm^{-3} $HClO_4$ solution.
Dashed line : net cation-exchanger phase absorption spectrum after subtracting the interstitial solution absorbance.

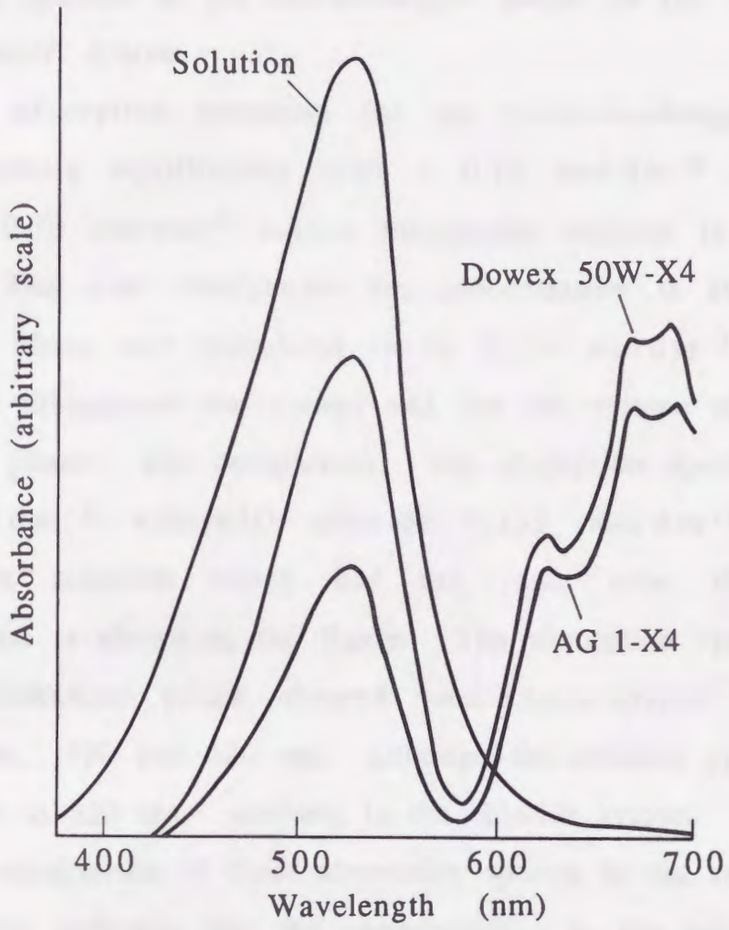

Fig. 3. Absorption spectra of the ion-exchanger phases and solution for the cobalt(II)-chloride system compared at the same ligand concentration (2.64 mol dm^{-3}).

Both cation- and anion-exchanger phase spectra had characteristic peaks at 520 nm (due to octahedral complexes) and 600 - 700 nm (due to tetrahedral complexes). On the other hand, the solution spectrum had a peak only at 520 nm. No peaks at longer wavelengths were observed.

Absorption spectra of the ion-exchanger phase in the cobalt(II)-*isothiocyanate system*

The absorption spectrum for the cation-exchanger Dowex 50W-X4 phase equilibrated with a 0.10 mol dm^{-3} cobalt(II) chloride - 0.70 mol dm^{-3} sodium thiocyanate solution is shown in Fig. 4. The total thiocyanate ion concentration in this cation-exchanger phase was calculated to be 0.155 mol dm^{-3} from the amount of thiocyanate ion sorbed and the net volume of the ion-exchanger phase. For comparison, the absorption spectrum of a 0.10 mol dm^{-3} cobalt(II) chloride - 0.155 mol dm^{-3} sodium thiocyanate solution which has the same total thiocyanate concentration is shown in the figure. The absorption spectrum for the ion-exchanger phase showed two characteristic peaks at wavelengths, 520 and 620 nm, although the solution again had a single peak at 520 nm, similarly to the chloride system.

The comparison of these absorption spectra at the same ligand concentration indicates that the complexibility in the ion-exchanger phase is intrinsically higher than that in the ordinary solution.

Determination of cation-exchanger corresponding solutions on complexation

In the foregoing sections, it was spectroscopically indicated that complexibility in the cation- or anion-exchanger solid phase is

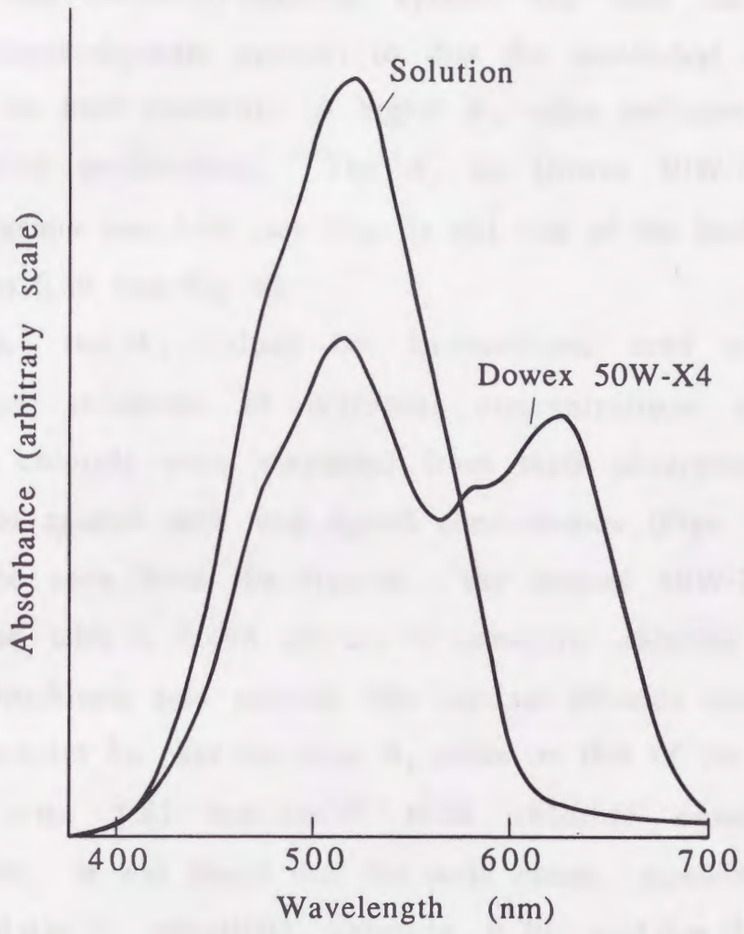

Fig. 4. Absorption spectra of the ion-exchanger phase and solution for the cobalt(II)-isothiocyanate system compared at the same ligand concentration (0.155 mol dm^{-3}).

much higher than in aqueous solutions of the same ligand concentration. Therefore, discussion will be made on what solution may correspond to the cation-exchanger phase in terms of complexation.

In comparing the complexation in different media, a spectral parameter A_r was conveniently introduced, which is defined as the ratio of absorbance at a wavelength for tetrahedral complexes (686 nm for the cobalt(II)-chloride system and 620 nm for the cobalt(II)-isothiocyanate system) to that for octahedral complexes (520 nm for both systems). A higher A_r value indicates a higher complexation environment. The A_r for Dowex 50W-X4 of the chloride system was 1.06 (see Fig. 3) and that of the isothiocyanate system was 0.89 (see Fig. 4).

Next, the A_r values for hydrochloric acid or sodium thiocyanate solutions of different concentrations containing cobalt(II) chloride were measured from their absorption spectra and plotted against each total ligand concentration (Figs. 5 and 6). As can be seen from the figures, the Dowex 50W-X4 phase, equilibrated with a 0.476 mol dm^{-3} cobalt(II) chloride - 5.4 mol dm^{-3} hydrochloric acid solution (the internal chloride concentration is 2.64 mol dm^{-3}), has the same A_r value as that of the cobalt(II) solution with 5.81 mol dm^{-3} total chloride concentration. Furthermore, it was found that the resin phase, equilibrated with 0.10 mol dm^{-3} cobalt(II) chloride - 0.70 mol dm^{-3} sodium thiocyanate solution (the internal thiocyanate concentration is 0.155 mol dm^{-3}), has the same A_r value as that of the cobalt(II) solution with 2.20 mol dm^{-3} total thiocyanate concentration. In all cases, the cation-exchange resin phase corresponded to a solution

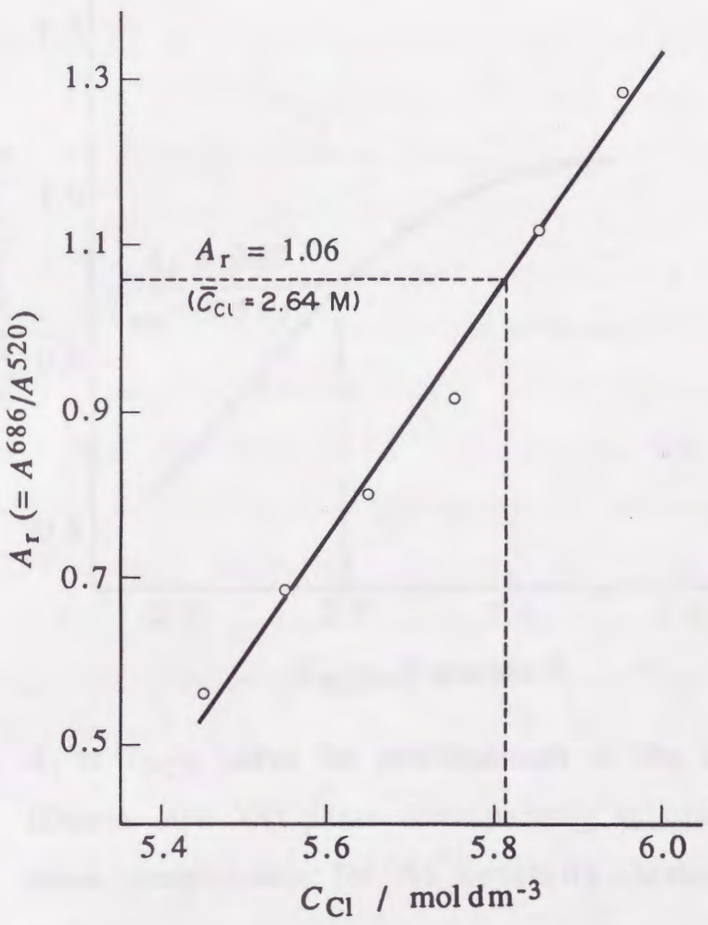

Fig. 5. A_r vs C_{Cl} curve for establishment of the ion-exchanger (Dowex 50W-X4) phase corresponding solution of the same complexation for the cobalt(II)-chloride system. C_{Cl} : total concentration of chloride ion.

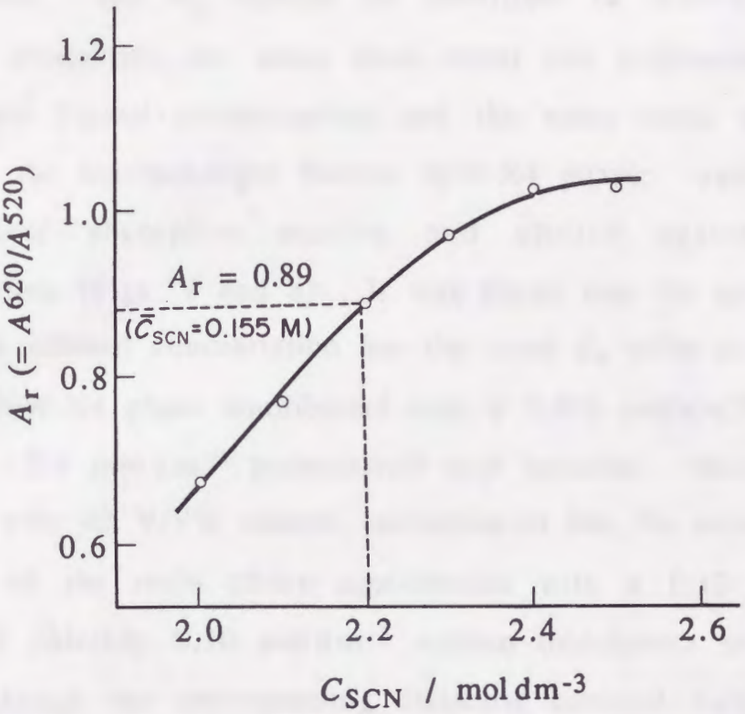

Fig. 6. A_r vs C_{SCN} curve for establishment of the ion-exchanger (Dowex 50W-X4) phase corresponding solution of the same complexation for the cobalt(II)-isothiocyanate system.

C_{SCN} : total concentration of thiocyanate ion.

with much higher ligand concentration in terms of complex formation.

One of the reasons for the higher complexibility of an ion-exchanger phase is considered to be its low dielectric constant due to the presence of organic components. To give an evidence for this assumption, the A_r values for solutions of different ethanol contents containing the same total metal ion concentration, the same total ligand concentration and the same ionic strength as those in the ion-exchanger Dowex 50W-X4 phase, were measured from their absorption spectra and plotted against ethanol concentration (Figs. 7 and 8). It was found that the solution with 51 V/V% ethanol concentration has the same A_r value as that of the Dowex 50W-X4 phase equilibrated with a 0.476 mol dm^{-3} cobalt(II) chloride - 5.4 mol dm^{-3} hydrochloric acid solution. Moreover, the solution with 43 V/V% ethanol concentration has the same A_r value as that of the resin phase equilibrated with a 0.10 mol dm^{-3} cobalt(II) chloride - 0.70 mol dm^{-3} sodium thiocyanate solution.

Although the corresponding dielectric constant value must be different depending on the electrolytes and solvents, the cation-exchanger Dowex 50W-X4 phase may approximately correspond to the solution containing 43 - 51 V/V% ethanol.

Method for evaluating the stability constant of a complex in the cation-exchanger phase

In order to give more quantitative explanation to the above observation that the complexibility in an ion-exchanger phase is higher than that in an ordinary aqueous solution, stability constants of a complex within cation-exchangers of different cross-

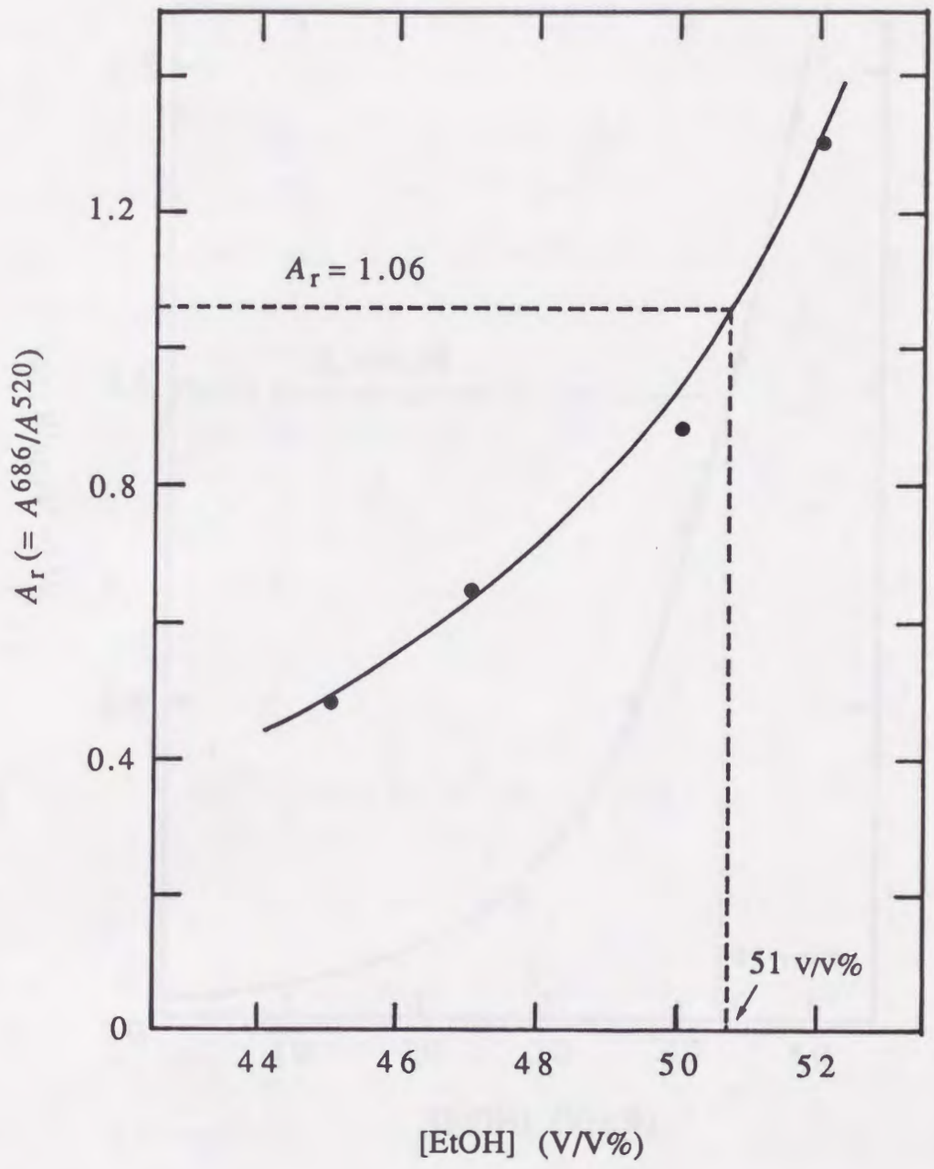

Fig. 7. A_r vs C_{Cl} curve for establishment of the ion-exchanger (Dowex 50W-X4) phase corresponding solution of the same complexation for the cobalt(II)-chloride system in the water-ethanol solution.

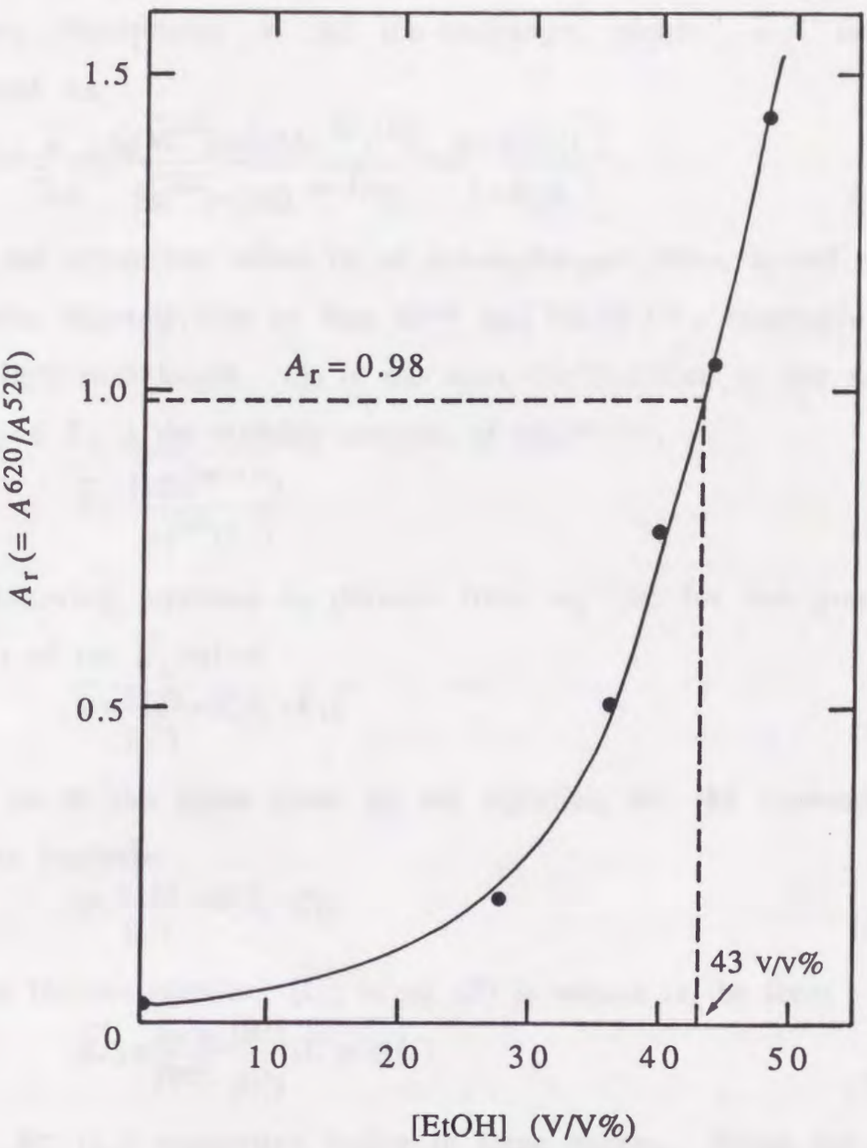

Fig. 8. A_r vs C_{SCN} curve for establishment of the ion-exchanger (Dowex 50W-X4) phase corresponding solution of the same complexation for the cobalt(II)-isothiocyanate system in the water-ethanol solution.

linking degrees were evaluated by a direct spectrophotometric technique.

When the reaction of M^{m+} and L^- forms only $ML^{(m-1)+}$, the apparent absorptivity in the ion-exchanger phase, $\bar{\varepsilon}$, can be expressed as

$$\bar{\varepsilon} \equiv \frac{\bar{A}}{C_M l} = \frac{\bar{\varepsilon}_0[\overline{M^{m+}}] + \bar{\varepsilon}_1[\overline{ML^{(m-1)+}}]}{[\overline{M^{m+}}] + [\overline{ML^{(m-1)+}}]} = \frac{\bar{\varepsilon}_0 + \bar{\varepsilon}_1 \bar{K}_1 [\overline{L^-}]}{1 + \bar{K}_1 [\overline{L^-}]}, \quad (3)$$

where the upper bar refers to an ion-exchanger phase, ε_0 and ε_1 are the molar absorptivities of free M^{m+} and $ML^{(m-1)+}$, respectively, l is the light path length, C_M is the total concentration of the sample metal and K_1 is the stability constant of $ML^{(m-1)+}$,

$$\bar{K}_1 = \frac{[\overline{ML^{(m-1)+}}]}{[\overline{M^{m+}}][\overline{L^-}]}. \quad (4)$$

The following equation is derived from eq. (3) for the graphical analysis of the $\bar{K}_1$ value.

$$\bar{\phi} \equiv \frac{\bar{\varepsilon} - \bar{\varepsilon}_0}{[\overline{L^-}]} = \bar{K}_1 \bar{\varepsilon}_1 - \bar{K}_1 \bar{\varepsilon} \quad (5)$$

which is of the same form as the equation for the conventional solution analysis:

$$\phi \equiv \frac{\varepsilon - \varepsilon_0}{[L^-]} = K_1 \varepsilon_1 - K_1 \varepsilon. \quad (6)$$

Using a Donnan relation, $[\overline{L^-}]$ in eq. (5) is written in the form

$$[\overline{L^-}] \equiv \frac{\gamma_{B^+}\gamma_{L^-}}{\bar{\gamma}_{B^+}\bar{\gamma}_{L^-}} \frac{[B^+]}{[\overline{B^+}]} [L^-] = k[L^-], \quad (7)$$

where B^+ is a supporting cation in large excess. When the ionic strength and the concentration of B^+ in the equilibrating solution are constant, $\bar{\gamma}_{B^+}$ or $\bar{\gamma}_{L^-}$ may also be constant as well as γ_{B^+} or γ_{L^-}. Thus, $[\overline{L^-}]$ can be evaluated by $[L^-]$ and a proportional constant k which had been determined using a known system. Accordingly, the stability constant of the one-to-one complex in the cation-

exchanger phase can be determined from the slope of $\bar{\phi}$ vs $\bar{\varepsilon}$ plots of eq. (5), in analogy to the ϕ vs ε plot for the solution analysis.

Evaluation of stability constants of the cobalt(II)*-isothiocyanate complex in the cation-exchanger phase*

The data necessary for evaluating the stability constants are listed in Table 1, where $\overline{[SCN^-]}$ was obtained using proportional constants in eq. (7), $k = 0.279$ (Dowex 50W-X2), 0.202 (-X4), 0.0837 (-X8) and 0.506 (SP-Sephadex C-25) which had been determined by a separate column equilibration experiment.

Ionic strength for the cation-exchanger phase, $\bar{I}$, was evaluated from the ion-exchange capacity and the amount of thiocyanate anion which invaded into the cation-exchanger phase in the absence of cobalt(II). The ionic strengths obtained for the ion-exchanger phase, which were expressed like an ordinary solution expression, were $\bar{I} = 1.7$ for Dowex 50W-X2, 2.0 for -X4, 3.4 for -X8 and 0.42 for SP-Sephadex C-25.

The graphical analyses for stability constants of the $CoNCS^+$ complex are shown in Fig. 9. For comparison, the stability constants of the same complex in aqueous solutions prepared so that the ionic strengths were the same as those within the ion-exchanger phase, were also determined. An example of the solution analysis is also given in Fig. 9. The stability constant values obtained are shown in Table 2.

As can be seen from the table, the stability constants for the cation-exchanger phase were always larger than those for the aqueous solution of the same ionic strength. One of the reasons is undoubtedly a low dielectric constant in the ion-exchanger phase due to the presence of organic components. Although the stability

Table 1. Data for evaluating stability constants of the $CoNCS^+$ complex in cation-exchanger phases

Dowex 50W-X2	$\bar{A}$	0.256	0.253	0.240	0.212	0.193	0.171
	$\bar{C}_{Co}$	0.452	0.360	0.285	0.234	0.200	0.174
	$[SCN^-]$	0	0.0236	0.0490	0.0754	0.102	0.129
Dowex 50W-X4	$\bar{A}$	0.315	0.321	0.297	0.267	0.231	0.203
	$\bar{C}_{Co}$	0.495	0.385	0.318	0.247	0.199	0.165
	$[SCN^-]$	0	0.0172	0.0357	0.0548	0.0743	0.0941
Dowex 50W-X8	$\bar{A}$	0.442	0.377	0.313	0.243	0.201	0.158
	$\bar{C}_{Co}$	0.751	0.587	0.461	0.353	0.277	0.210
	$[SCN^-]$	0	0.0071	0.0147	0.0226	0.0307	0.0388
SP-Sephadex C-25	$\bar{A}$	0.056	0.108	0.131	0.136	0.137	0.138
	$\bar{C}_{Co}$	0.155	0.132	0.119	0.110	0.100	0.090
	$[SCN^-]$	0	0.0344	0.0716	0.110	0.149	0.189

Equilibrating solutions are $NaSCN + NaClO_4$ ($I = 0.5$) containing 0.05 M $Co(ClO_4)_2$. The absorbance for the ion-exchanger phase is taken as $\bar{A} = \bar{A}^{514} - \bar{A}^{570}$, $\bar{C}_{Co}$ was obtained by dividing the total amount of cobalt(II) sorbed by the net volume of ion-exchanger phase, expressed in mol dm^{-3}.

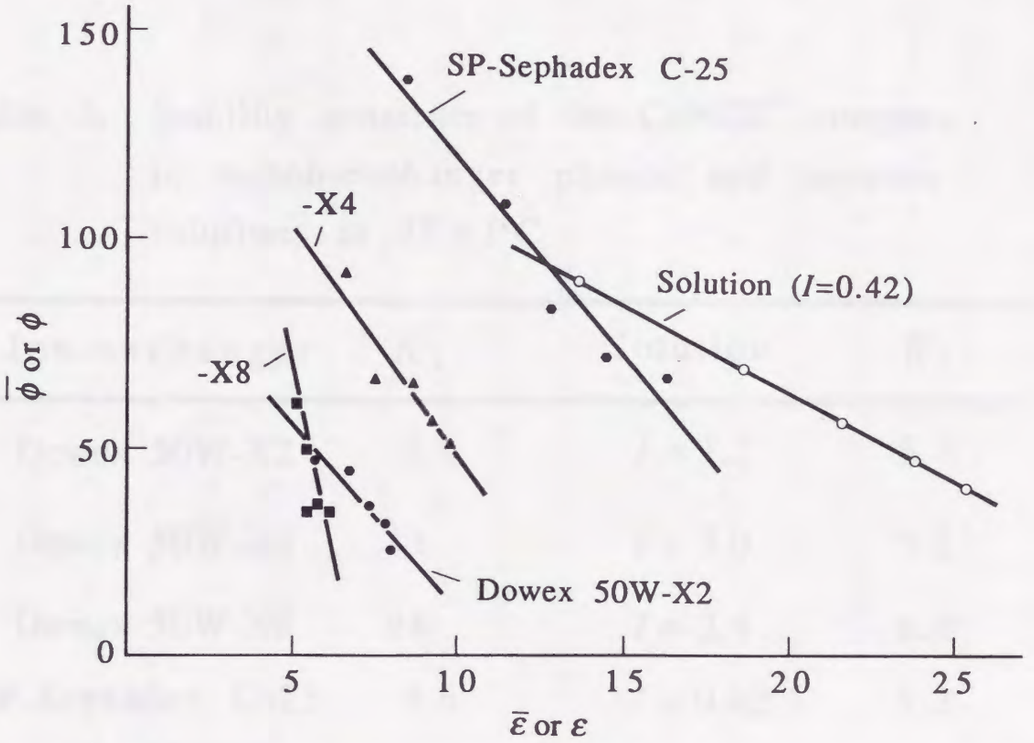

Fig. 9. Determination of stability constants of the one-to-one cobalt(II)-isothiocyanate complex in cation-exchanger phases and aqueous solutions at 25±1℃.

Table 2. Stability constants of the $CoNCS^+$ complex in cation-exchanger phases and aqueous solutions at $25 \pm 1°C$

Ion-exchanger	$\overline{K}_1$	Solution	K_1
Dowex 50W-X2	8.9	$I = 1.7$	5.3
Dowex 50W-X4	11	$I = 2.0$	5.2
Dowex 50W-X8	28	$I = 3.4$	6.0
SP-Sephadex C-25	9.6	$I = 0.42$	5.3

constant for the aqueous solution was nearly constant, irrespective of ionic strength, the constant for the cation-exchange resin increased with an increase in the degree of cross-linking, namely, with an increase in ionic strength.

Another reason for the higher complexibility in the ion-exchanger phase may be the presence of a high internal pressure produced by the resin network. When the following reaction occurs in the ion-exchange resin,

$$Co^{2+}(aq) + NCS^{-}(aq) \rightleftharpoons CoNCS^{+}(aq) + nH_2O \qquad (8)$$

some of the solvated water molecules are liberated through the complexation reaction and excluded from the resin phase. When water molecules are transferred to the solution phase from the highly-pressured ion-exchange resin phase, the energy $\pi\Delta V$ is released where π is the swelling pressure and ΔV is the volume contraction of the resin phase through the reaction. The higher the degree of cross-linking, the higher the internal pressure and the larger $\pi\Delta V$; thus the complexation increases.

In spite of the lower internal pressure and the lower ionic strength of SP-Sephadex C-25 compared with the ion-exchange resins, the stability constant for SP-Sephadex C-25 is found to be somewhat larger than that for Dowex 50W-X2. This could be due to an attractive interaction between the thiocyanate ion and the aromatic ring of the Dowex resins. Such a π-π interaction may somewhat weaken the ligand activity of the thiocyanate ion.

In any case, the fact that the cation-exchanger renders the high complexation ability should be sufficiently taken into consideration when using conventional cation-exchange methods for evaluating stability constants, where complexation with anionic

ligands in the cation-exchanger phase has frequently been neglected for simplification without evidence.[9,10]

CHAPTER 2. ^{31}P NMR SPECTROSCOPIC STUDIES ON COMPLEXATION EQUILIBRIA OF CADMIUM(II)-PHOSPHINATE COMPLEXES IN CATION-EXCHANGERS

INTRODUCTION

An ion-exchanger internal phase can be regarded as a concentrated and heterogeneous polyelectrolyte solution in point of chemical reactivity of ions.[11,12] The knowledge on complexation in such a special kind of solution must be important for understanding chemical reactions in biological media,[13] however, the complexation equilibria of ions sorbed into the ion-exchangers had not sufficiently been discussed yet. It is only known that a very high complexation of metal ions in the anion-exchanger phase is due to the high ligand anion concentration and that a very low complexation in the cation-exchanger is due to the exclusion of ligand anions. It was considered, however, that there should also be other factors influencing complexation reactions in the ion-exchanger phase, such as dielectric constant, internal pressure and ionic mobility. One of the reasons for the lack of information on the complexation equilibria in the ion-exchanger solid phase may be that there are difficulties in the precise measurement of such solid particle samples.

The previous chapter treated the absorption spectroscopic studies on complexation equilibria of inorganic cobalt(II) complexes in ion-exchangers. The stabilities of complexes in the cation-exchanger phase were always higher than those in the

corresponding solution, indicating that the ion-exchanger has complexation enhancing effects due to low dielectric constant and high internal pressure.

In order to make the same type of comparison, this chapter will deal with ^{31}P NMR spectroscopic studies on complexation equilibria for a labile cadmium(II)-phosphinate complex system in cation-exchanger phases and in aqueous solutions. Stability constants for the Cd^{2+}-$PH_2O_2^-$ complex system in the ion-exchanger phase and in the solution[1-4] are reported as the first data.

EXPERIMENTAL

Chemicals

All reagents used were of commercially available reagent grade. Strong acid-type cation-exchange resins of different cross-linking degrees, Muromac AG (purified "Dowex") 50W-X2, -X4 and -X8 (100-200 mesh), of the sodium form; a strong base-type anion-exchange resin, Muromac AG 1-X4 (100 - 200 mesh), of the chloride form; and a cross-linked dextran gel-type cation-exchanger, SP-Sephadex C-25 (Pharmacia, Uppsala, Sweden) of the sodium form; were used.

Batch distribution experiment

An appropriate amount of the dry cation-exchanger (e.g. 0.8 g for AG 50W-X2, 1.2 g for -X4, 1.8 g for -X8 and 0.5 g for SP-Sephadex C-25) was equilibrated with 20 cm^3 of a solution containing $Cd(ClO_4)_2$, $NaPH_2O_2$ and $NaClO_4$ in a stoppered test tube at room temperature for 3 - 6 h. The compositions of the solutions

are listed in Table 3. After equilibration, cadmium(II) and phosphinate in the equilibrated solution were analysed. Cadmium(II) was determined by EDTA titration and phosphinate was determined spectrophotometrically with a molybdenum(V)-molybdenum(VI) reagent.[14]

Table 3. Compositions of solutions prepared for the batch equilibration

Medium	C_{Cd} (mol dm^{-3})	C_P (mol dm^{-3})	C_{Na} (mol dm^{-3})
AG 50W-X2	0.04 - 0.08	0.15	0.25
-X4	0.13	0.1 - 0.5	0.5
-X8	0.26	0.2 - 1.0	1.0
SP-Sephadex C-25	0.005 - 0.025	0.05	0.05

C_{Cd}, C_P and C_{Na} : tatal concentrations of cadmium, phosphinate and sodium.

NMR measurements

The NMR spectra were recorded on a JEOL JNM-GX 400 spectrometer at probe temperature of 22.5(±1) °C.

^{31}P NMR spectra were recorded at 161.858 MHz. The NMR parameters were chosen so that quantitative analysis was possible: a flip angle of ~90 ° (20.0 μs), pulse repetition time 3 s, spectral width ~6500 Hz and scan accumulation number 40 - 1000 for enhancement in the S/N ratio. The chemical shifts were reported with respect to 85 % H_3PO_4 as an external reference. A 10 mm I.D. sample tube was employed and the field/frequency lock was achieved with the ^2H resonance of D_2O contained in a 2 mm tube.

Proton NMR spectra were recorded at 399.782 MHz. The NMR parameters were typical flip angle ~45 ° (7.9 μs), pulse repetition time 5 s, spectral width 400 Hz and scan accumulation number 8.

The chemical shifts were reported in ppm with respect to H_2O as an external reference. A 5 mm I.D. sample tube was employed.

NMR spectra for an ion-exchanger phase were recorded as follows. The ion-exchanger beads sorbing sample species were packed into 10 or 5 mm NMR sample tubes with a small amount of equilibrated solution and allowed to settle to a height of about 4.5 cm. The NMR spectra for the ion-exchanger bed were recorded in the same way as that for an ordinary solution. Thus, the observed NMR spectrum for the ion-exchanger bed contained both signals in the ion-exchanger phase and the interstitial equilibrated solution.

The sample tube containing only solution was rotated, but the tube containing ion-exchanger beads was not rotated during NMR measurements. The integral spectral intensity was obtained by weighing the cut-out paper corresponding to the peak area recorded.

Determination of volume and ionic concentrations for an ion-exchanger phase

Volume fractions of the ion-exchanger internal solution (R_i), the skeleton (R_k) and the interstitial solution (R_s) in an NMR sample tube were determined from ^1H and ^{31}P NMR signal intensities. In this treatment, the net volume of the ion-exchanger phase was taken as the volume including both the internal solution and the organic skeleton. Thus, the net volume of the ion-exchanger phase, $\overline{V}$, can be calculated from the apparent bed volume (V).

$$\overline{V} = (R_i + R_k)V \qquad (9)$$

The total cadmium(II) concentration in the ion-exchanger phase, $\overline{C}_{Cd}$, was calculated from the difference between its initial (m_{Cd}^{int})

and equilibrium (m_{Cd}^{eq}) amounts in the solution and from the net volume of the ion-exchanger phase.

$$\bar{C}_{Cd} = \frac{m_{Cd}^{int} - m_{Cd}^{eq}}{\bar{V}} \qquad (10)$$

The total phosphinate concentration in the ion-exchanger phase, $\bar{C}_P$, was calculated from the phosphinate concentration in the equilibrated solution (C_P^{eq}), the volume fractions and the ^{31}P NMR signal intensities for the ion-exchanger phase ($\bar{A}$) and the interstitial solution (A_S).

$$\bar{C}_P = \frac{\bar{A}}{A_s} \frac{R_s}{R_i + R_k} C_P^{eq} \qquad (11)$$

All concentrations of ions for the solid phase were expressed in mol dm^{-3}, like an ordinary solution expression. Ionic strength for the cation-exchanger phase, $\bar{I}$, was evaluated from the ion-exchange capacity and the amount of phosphinate anion which invaded into the cation-exchanger phase in the absence of cadmium(II). All ionic strengths for the solid phases were also expressed like an ordinary solution expression.

RESULTS AND DISCUSSION

^{31}P NMR chemical shift in the ion-exchanger phase

The ^{31}P NMR spectra of phosphinate anion $PH_2O_2^-$ sorbed into cation- and anion-exchangers were recorded and compared with the spectra of the anion in the interstitial equilibrated solution (Fig. 10). The ^{31}P signal in the cation-exchanger 50W-X4 shifted lowfield while that in the anion-exchanger 1-X4 shifted highfield relative to that in the equilibrated solution. The magnitude of the shift upon an interaction with the anion-exchanger was larger than

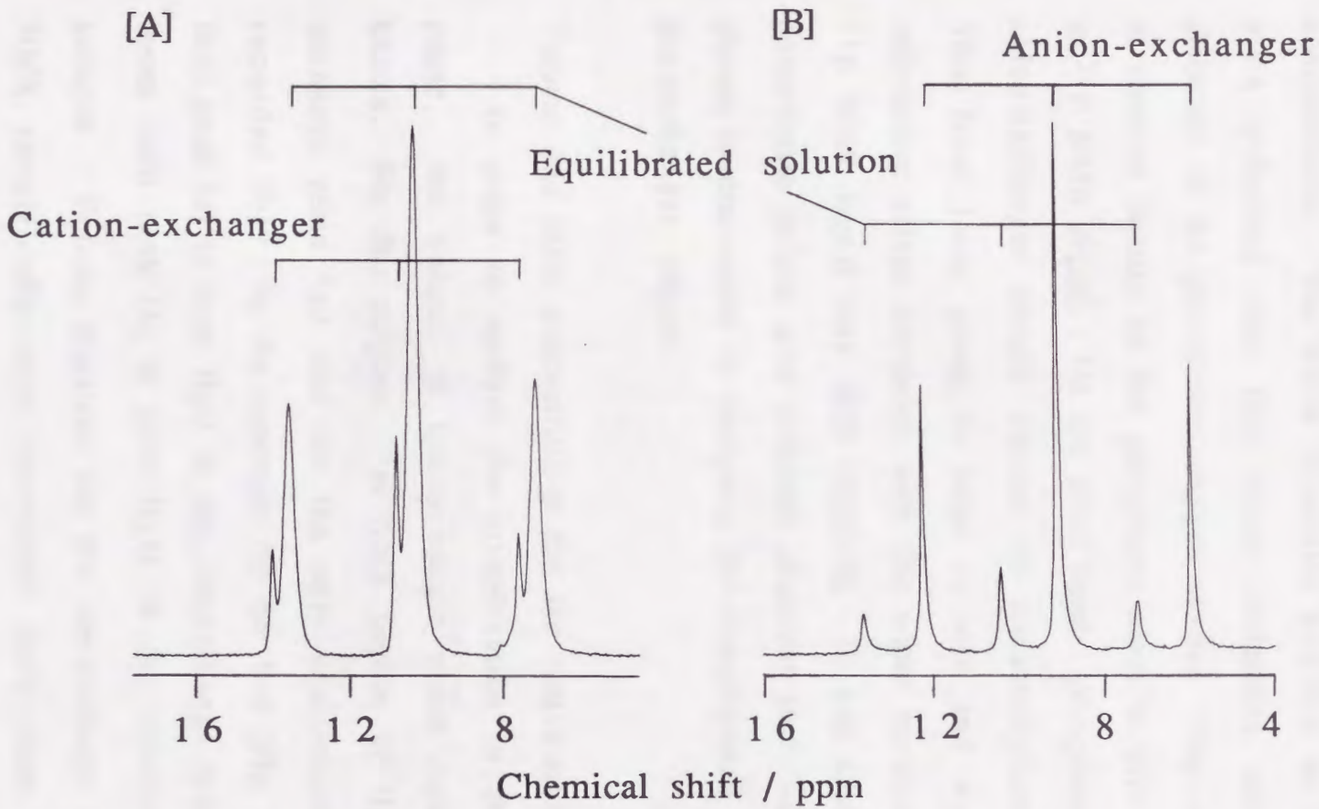

Fig. 10. ^{31}P NMR spectra of phosphinate ion for cation- and anion-exchanger phases;
[A] Muromac AG 50W-X4 and [B] Muromac AG 1-X4 equilibrated with 0.5 mol dm^{-3} $NaPH_2O_2$ or 0.1 mol dm^{-3} $NaPH_2O_2$-$NaNO_3$ solution (pH 7).

the cation-exchanger. The phosphinate anions present in the cation-exchanger may contact to hydrated ions (such as Na^+) in high concentration. The water molecules hydrated to sodium ions are more polarized than free water molecules and thus subtract electrons of the phosphinate oxygen atoms. This causes a lowering in electron density on the phosphorus atom to give a lowfield shift in ^{31}P NMR signal. On the other hand, phosphinate anions in the anion-exchanger should contact to tetramethylammonium groups. This fixed ionic group is large in size and weak in electron-subtracting effect compared with the water molecule. Thus, the ^{31}P NMR signal may shift highfield. In any case, the fact that phosphinate anions give different chemical shift values in different phases is convenient in analysing the complexation equilibria in the ion-exchanger phases.

Volume and ionic concentrations for the cation-exchanger phase

In order to analyse the complexation in the ion-exchanger phase, the volume of ion-exchanger phase concerned must be known. For this purpose, ^1H NMR spectra of H_2O for a cation-exchange resin bed and for the only equilibrated solution were recorded.[15,16] In the spectrum for the bed (Fig. 11), the higher field peak (a) is from H_2O in the ion-exchange resin phase and the lower field peak (b) is from H_2O in the interstitial equilibrated solution. Volume fractions for the ion-exchange resin bed in an NMR sample tube were determined from these peak intensities (Table 4). The volume fraction of the gel skeleton for a SP-Sephadex C-25 bed in the NMR sample tube was also obtained from ^1H NMR peak intensities in the same way as those for resins, while the fraction of the interstitial solution was obtained from ^{31}P NMR

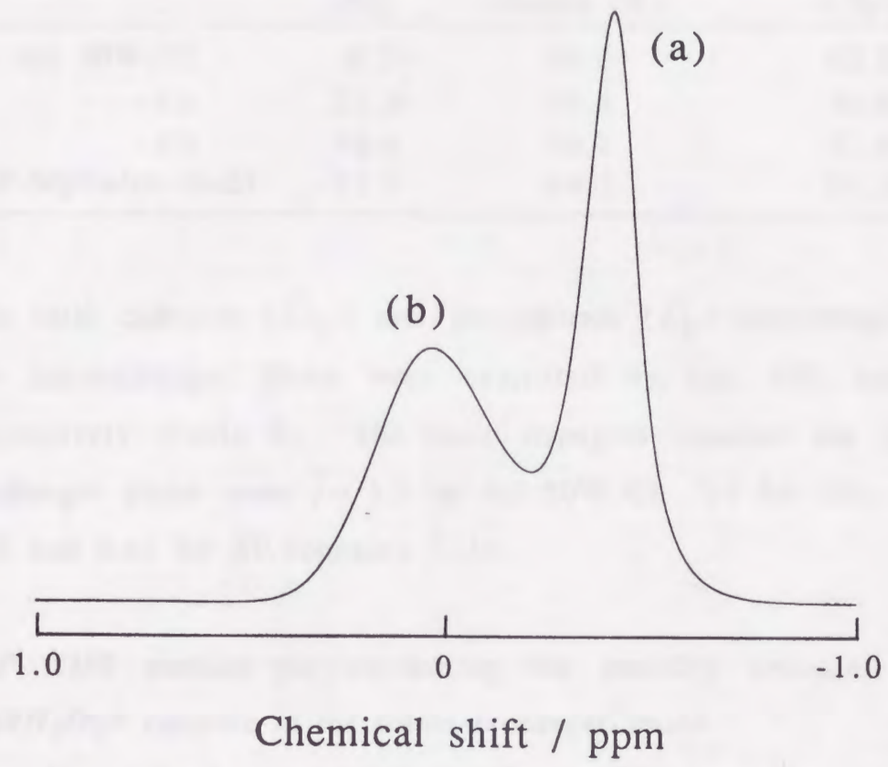

Fig. 11. ^1H NMR spectrum for a cation-exchanger (AG 50W-X8) bed equilibrated with an $NaPH_2O_2$ (1.0 mol dm^{-3}) solution;
(a) ion-exchanger phase and (b) interstitial equilibrated solution.

peak intensities of phosphinate anion in a sample solution with and without the gel (Table 4), because ^1H signal for the gel phase could not be observed separately from that for the interstitial solution.

Table 4. Volume fractions for an ion-exchanger bed in an NMR sample tube

Medium	Skeleton (%)	Resin internal solution (%)	Interstitial solution (%)
AG 50W-X2	9.3	58.3	32.2
-X4	21.2	53.4	25.4
-X8	46.4	29.1	23.9
SP-Sephadex C-25	12.7	64.1	23.2

The total cadmium ($\bar{C}_{Cd}$) and phosphinate ($\bar{C}_P$) concentrations in the ion-exchanger phase were evaluated by eqs. (10) and (11), respectively (Table 5). The ionic strengths obtained for the ion-exchanger phase were $\bar{I}$ = 1.2 for AG 50W-X2, 2.0 for -X4, 2.9 for -X8 and 0.45 for SP-Sephadex C-25.

^{31}P NMR method for evaluating the stability constant of the $CdPH_2O_2^+$ complex in the cation-exchanger phase

If the ligand exchange of cadmium(II) complexes in an ion-exchanger phase is sufficiently rapid relative to the NMR time-scale, a single time-averaged ^{31}P peak appears and the position should be given by:

$$\bar{\delta}_{obs} = \Sigma \bar{\delta}_i \bar{X}_i ; \qquad (12)$$

where the upper bar refers to an ion-exchanger phase, δ_{obs} is the observed chemical shift, δ_i is the chemical shift of $Cd(PH_2O_2)_i^{(2-i)+}$ and X_i is the mole fraction of the i-th species. When the reaction of Cd^{2+} and $PH_2O_2^-$ forms only $CdPH_2O_2^+$ in a cation-exchanger phase,

Table 5. Data for evaluating stability constants of the $CdPH_2O_2^+$ complex in cation-exchanger phases

Ion-exchanger	$\bar{C}_{Cd}$ (mol dm^{-3})	$\bar{C}_P$ (mol dm^{-3})	$\bar{\delta}_{obs}$ (ppm)
AG 50W-X2	0	0.0278	10.51
	0.209	0.0681	11.71
	0.255	0.0746	11.93
	0.293	0.0821	12.08
	0.337	0.0930	12.27
	0.373	0.0982	12.38
AG 50W-X4	0	0.0352	10.69
	0.493	0.0307	13.73
	0.454	0.0572	13.53
	0.418	0.0776	13.35
	0.382	0.0953	13.17
	0.351	0.109	12.98
AG 50W-X8	0	0.0302	10.90
	0.740	0.0465	15.32
	0.638	0.0706	15.00
	0.549	0.0823	14.67
	0.447	0.0940	14.29
	0.374	0.100	13.91
SP-Sephadex C-25	0	0.0036	10.32
	0.0345	0.0050	10.74
	0.0659	0.0066	11.05
	0.0900	0.0086	11.28
	0.111	0.0099	11.45
	0.128	0.0114	11.57

$\bar{C}_{Cd}$: total cadmium concentration in the ion-exchanger phase.

$\bar{C}_P$: total phosphinate concentration in the ion-exchanger phase.

the observed ^{31}P chemical shift in the ion-exchanger phase, $\bar{\delta}_{obs}$, can be expressed as:

$$\bar{\delta}_{obs} = \frac{\bar{\delta}_o[\overline{PH_2O_2^-}] + \bar{\delta}_1[\overline{CdPH_2O_2^+}]}{[\overline{PH_2O_2^-}] + [\overline{CdPH_2O_2^+}]} = \frac{\bar{\delta}_o + \bar{\delta}_1\bar{K}_1[\overline{Cd^{2+}}]}{1 + \bar{K}_1[\overline{Cd^{2+}}]}; \quad (13)$$

where $\bar{K}_1$ is the stability constant of $CdPH_2O_2^+$ in the ion-exchanger phase:

$$\bar{K}_1 = \frac{[\overline{CdPH_2O_2^+}]}{[\overline{Cd^{2+}}][\overline{PH_2O_2^-}]}. \quad (14)$$

The following equation is derived from eq. (13) for the analysis of the $\bar{K}_1$ value.

$$\frac{\bar{\delta}_{obs} - \bar{\delta}_o}{[\overline{Cd^{2+}}]} = -\bar{K}_1\bar{\delta}_{obs} + \bar{\delta}_1\bar{K}_1 \quad (15)$$

Therefore, the stability constant of the one-to-one complex in the cation-exchanger phase, $\bar{K}_1$, can be determined from the slope of the $(\bar{\delta}_{obs} - \bar{\delta}_o)/[\overline{Cd^{2+}}]$ vs $\bar{\delta}_{obs}$ plot. The ^{31}P chemical shift value characteristic to the $CdPH_2O_2^+$ complex in the cation-exchanger phase, $\bar{\delta}_1$, can be determined from the intercept of the plots. The same type of analysis was also applied to ordinary solutions for comparison.

Evaluation of stability constants of the cadmium(II)*-phosphinate complex in the cation-exchanger phase*

For the purpose of comparing complexbilities in an ion-exchanger phase and in an ordinary aqueous solution, stability constants of the $CdPH_2O_2^+$ complex within cation-exchangers were evaluated.

A ^{31}P NMR spectrum for the cation-exchanger bed equilibrated with a solution containing cadmium(II) and phosphinate is shown in Fig. 12. The triplet signal (a) at a lower field is assigned to phosphinate in the ion-exchanger phase and the

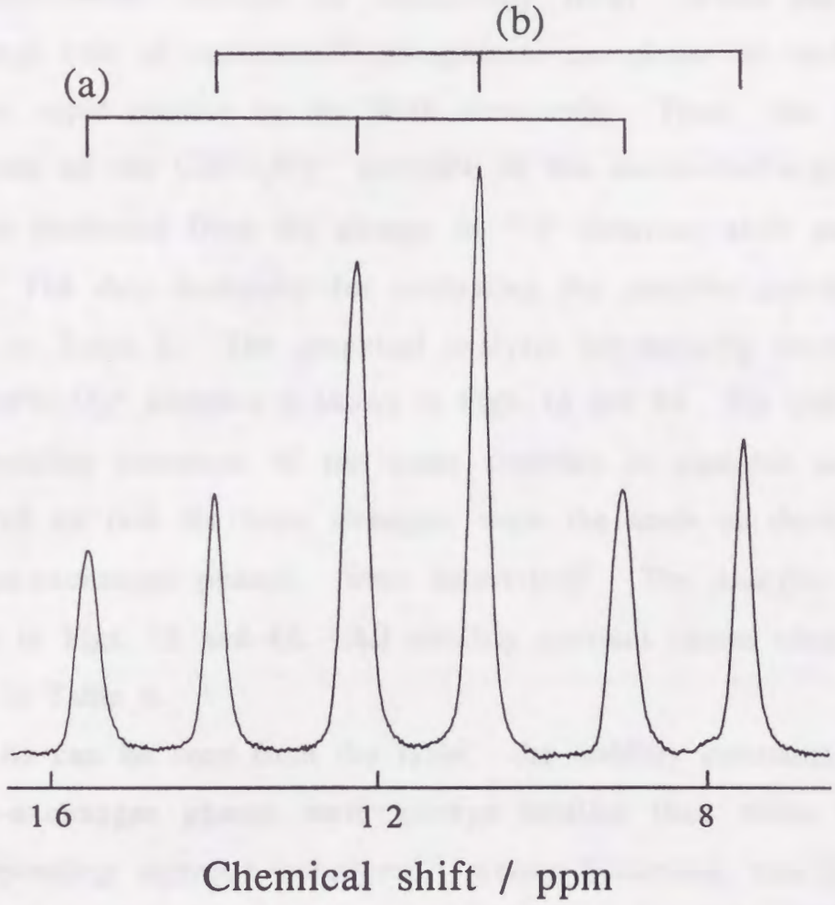

Fig. 12. ^{31}P NMR spectrum for a cation-exchanger (AG 50W-X2) bed equilibrated with a $Cd(ClO_4)_2$ (0.08 mol dm^{-3}), $NaPH_2O_2$ (0.15 mol dm^{-3}) and $NaClO_4$ (0.1 mol dm^{-3}) solution;
(a) ion-exchanger phase and (b) interstitial equilibrated solution.

triplet signal (b) at a higher field to that in the interstitial equilibrated solution. It may be considered that the ion exchange rate of the chemical species between the ion-exchanger phase and the equilibrated solution is sufficiently slow, while the ligand exchange rate of cadmium(II)-phosphinate complexes in each phase is very rapid relative to the NMR time-scale. Thus, the stability constants of the $CdPH_2O_2^+$ complex in the cation-exchanger phase can be evaluated from the change in ^{31}P chemical shift using eq. (15). The data necessary for evaluating the stability constants are listed in Table 5. The graphical analysis for stability constants of the $CdPH_2O_2^+$ complex is shown in Figs. 13 and 14. For comparison, the stability constants of the same complex in aqueous solutions, prepared so that the ionic strengths were the same as those within the ion-exchanger phases, were determined. The analysis is also shown in Figs. 13 and 14. All stability constant values obtained are given in Table 6.

As can be seen from the table, the stability constants for the cation-exchanger phases were always smaller than those for the corresponding aqueous solutions, whose behaviour was different from those for the $CoNCS^+$ (**CHAPTER 1**) and $AlPH_2O_2^{2+}$ complexes.[17] It was found that the cation-exchanger rendered not only complexation enhancing effects but also lowering effects. For the $CdPH_2O_2^+$ complex, the complexation lowering effect due to low ionic mobility and spatial restriction may be predominant over the enhancing effect due to low dielectric constant and high internal pressure.

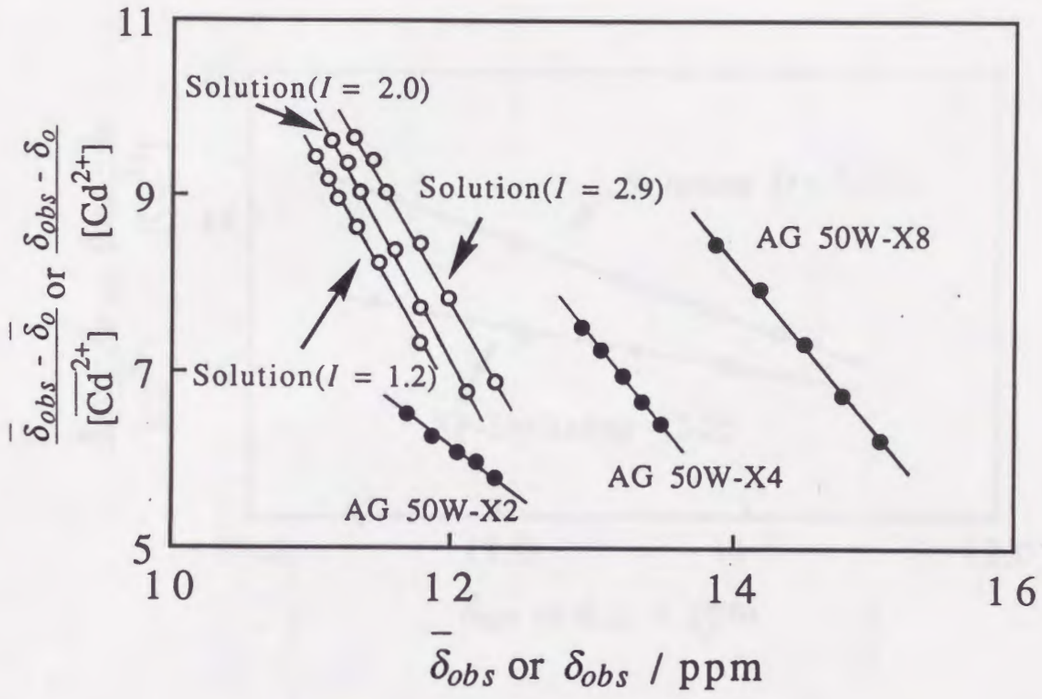

Fig. 13. Determination of stability constants of the $CdPH_2O_2^+$ complex in the cation-exchange resin phase and the corresponding aqueous solution by ^{31}P NMR method.

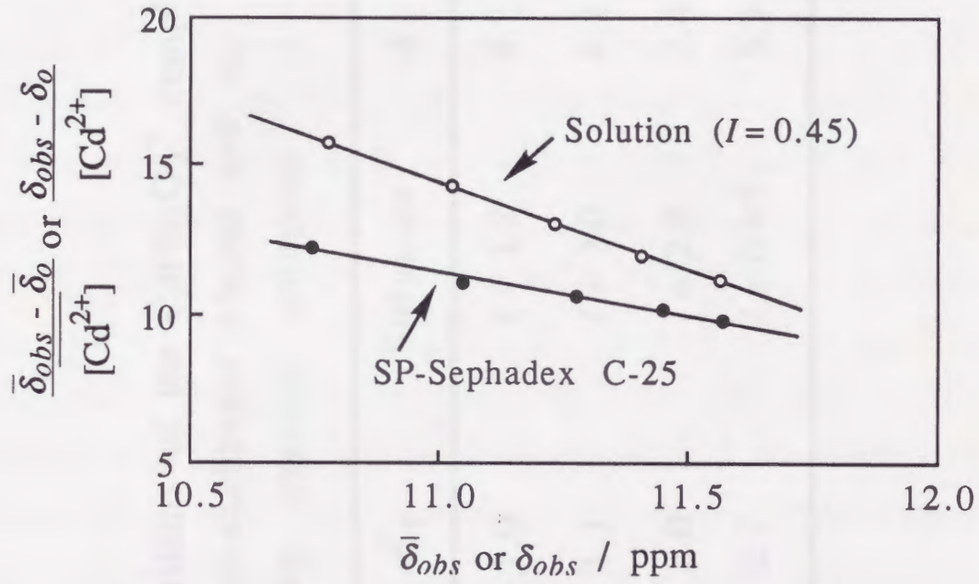

Fig. 14. Determination of stability constants of the $CdPH_2O_2^+$ complex in the cation-exchanger phase and the corresponding aqueous solution by ^{31}P NMR method.

Table 6. Stability constants of the $CdPH_2O_2^+$ complex in the cation-exchanger phases and the corresponding aqueous solutions

Ion-exchanger	$\overline{K}_1$	Solution	K_1
AG 50W-X2	1.0	$I = 1.2$	6.8
AG 50W-X4	1.1	$I = 2.0$	6.2
AG 50W-X8	2.0	$I = 2.9$	7.4
SP-Sephadex C-25	2.7	$I = 0.45$	5.9

Comparison of ^{31}P chemical shifts between the cation-exchanger phase and the corresponding solution

From the intercept of the $(\bar{\delta}_{obs} - \bar{\delta}_o)/[\overline{Cd^{2+}}]$ vs $\bar{\delta}_{obs}$ plot of eq. (15), the ^{31}P chemical shift values of the $CdPH_2O_2^+$ complex in the cation-exchanger phases can be obtained. The values are summarised in Table 7, as well as those for the corresponding solutions. The values for the free phosphinate ion, $BePH_2O_2^+$ and $AlPH_2O_2^{2+}$ complexes in both phases are also listed in Table 7 for comparison. The ^{31}P chemical shift values of free phosphinate ion, $BePH_2O_2^+$ and $AlPH_2O_2^{2+}$ complexes in the cation-exchanger phases were not appreciably different from those in the corresponding aqueous solutions. On the other hand, the values of the $CdPH_2O_2^+$ complex in the cation-exchanger phases were lowfield compared to those in the corresponding aqueous solutions. This fact may indicate that the coordination environment and hydration state of the $CdPH_2O_2^+$ complex in the cation-exchanger phase are clearly different from those in the solution. When a phosphinate ion coordinates strongly to the cadmium ion, a large lowfield shift of ^{31}P NMR signal relative to the signal of the free phosphinate ion is expected. The fact that the chemical shift of the complex in the cation-exchanger phase is more lowfield than that in the corresponding aqueous solution may be explained by the change in the binding form. The following intramolecular equilibrium between chelate and non-chelate forms can exist for the phosphinate complex.[18,19]

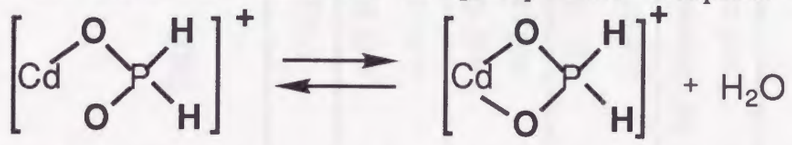

Non-Chelate Chelate (16)

Of the two binding forms, the ^{31}P chemical shift for the chelate form should be more lowfield than that for the non-chelate form.

Table 7. ^{31}P chemical shift values for phosphinate complexes in cation-exchanger phases and the corresponding aqueous solutions

Medium	Ionic strength	$PH_2O_2^-$	$CdPH_2O_2^+$	$BePH_2O_2^+$	$AlPH_2O_2^{2+}$
AG 50W-X2	1.2	10.5	17.6	8.9	6.9
solution		10.8	14.1	9.3	6.9
AG 50W-X4	2.0	10.7	19.4	9.0	7.1
solution		11.1	14.9	9.5	7.0
AG 50W-X8	2.9	10.9	18.4	9.0	7.3
solution		11.4	15.4	9.6	7.1
SP-Sephadex C-25	0.45	10.3	15.3		
solution		10.5	15.2		

Chemical shift is expressed in ppm with respect to 85% H_3PO_4.

The species sorbed into an ion-exchanger phase should be somewhat dehydrated and the liberated water molecules may be transferred to the external solution from the highly-pressured ion-exchanger phase to stabilise the system. Therefore, the chelate form which is more dehydrated than the non-chelate form is more favoured in the ion-exchanger phase than in the corresponding aqueous solution. This tendency may be more pronounced for an ion-exchanger of a higher cross-linking degree, where higher hydrophobicity and higher internal pressure are effective.

On the other hand, the $BePH_2O_2^+$ and $AlPH_2O_2^{2+}$ complexes may have almost wholly the chelate form in both ion-exchangers and solutions, thus the ^{31}P chemical shift values of these complexes are similar for ion-exchangers and solutions.

In any case, the NMR method mentioned above is a very powerful one in the analysis of the complexation equilibria in the ion-exchanger phase. It was found that ion-exchangers rendered complexation lowering effect as well as enhancing effect due to their characteristic properties.

CHAPTER 3. ^{11}B NMR SPECTROSCOPIC STUDIES ON COMPLEXATION EQUILIBRIA OF BORATE-DIHYDROXYCARBOXYLATE COMPLEXES IN ANION-EXCHANGE RESINS

INTRODUCTION

In an aqueous solution, many polyhydroxy compounds react with borate ions ($B(OH)_4^-$) forming 1:1 and 1:2 complexes[20-22] according to the reactions

$$B^- + L \rightleftharpoons BL^- + 2H_2O \qquad K_1 \qquad (17)$$

$$BL^- + L \rightleftharpoons BL_2^- + 2H_2O \qquad K_2 \qquad (18)$$

where B^-, L, BL_n^- and K_n stand for $B(OH)_4^-$, polyhydroxy ligand, the 1:n complex formed and the stability constants of the complex, respectively. At pH > 11, B^- is the preponderant ion in an aqueous solution of sodium borate; at lower pH, it is converted, at least in part, into boric acid, B, and the equilibrium

$$B + OH^- \rightleftharpoons B^- \qquad pK_a = 8.98 \qquad (19)$$

becomes important.[23] Formation of polyborates also becomes important in a concentrated solution (more than 0.025 mol dm^{-3}) at pH 8 - 11.[24] The complexation among borate ions and hydroxy compounds in an aqueous solution has been investigated by using ^{11}B NMR spectroscopy.[20-22] Since the reaction rate of eq. (17) or (18) is slow relative to the NMR time scale, ^{11}B signals can be observed independently for each species.

In analytical use, anion-exchangers of the $B(OH)_4^-$ form were successfully applied to the separation of polyhydroxy compounds,

such as sugars.[25,26] Nevertheless, little has been known on the complexation equilibria of species sorbed into the ion-exchanger.

In the previous chapters, complexation equilibria between ions with opposite charge (cation-anion) in the ion-exchanger phase were dealt. This chapter will treat complexation equilibria between ions with the same charge (anion-anion), such as borate-dihydroxycarboxylate, in the anion-exchange resin phase investigated by using ^{11}B NMR spectroscopy. Some authors[27,28] reported charge-transfer reactions between ions with the same charge sorbed into ion-exchangers, however, complexation equilibria between them had not sufficiently been discussed yet.

EXPERIMENTAL

Chemicals

All reagents used were of commercially available reagent grade. Strong base-type anion-exchange resins of different cross-linking degrees, Dowex 1-X2, Bio-Rad AG 1-X4 and Muromac AG 1-X8 (100 - 200 mesh), of the chloride form were used.

Preparation of samples for ^{11}B NMR

Anion-exchange resin samples for ^{11}B NMR measurements were prepared as follows. An appropriate amount of the dry anion-exchanger (e.g. 0.9 g for 1-X2, 1.1 g for 1-X4 and 1.6 g for 1-X8) was equilibrated with 20 cm^3 of a 5×10^{-4} mol dm^{-3} borate solution (pH 11.5) containing $(3.0 - 4.4) \times 10^{-3}$ mol dm^{-3} glycerate or $(4.0 - 6.0) \times 10^{-3}$ mol dm^{-3} tartrate in a stoppered test tube at room temperature for 3 - 6 h. The pH value of the solution was adjusted

to pH 11.5 with a small amount of sodium hydroxide solution. These weak acids in the solution were fully deprotonated and all of the ions were sorbed into the anion-exchanger under the experimental condition. The total concentration of borate in the anion-exchanger phase was adjusted to be less than 0.005 mol per one dm^3 of resin phase volume to avoid the formation of polyborates.

For the solution samples, a 0.01 mol dm^{-3} borate solution containing glycerate or tartrate was prepared at a given ionic strength using tetramethylammonium chloride. The pH value of the solution was adjusted to pH 12 with a small amount of sodium hydroxide solution. The NMR spectrum was recorded in the conventional way.

NMR measurements

The NMR spectra were recorded on a JEOL JNM-GX 400 spectrometer at probe temperature of 22.5(±1) °C.

^{11}B NMR spectra were recorded at 128.262 MHz. The NMR parameters were chosen so that quantitative analysis was possible: a flip angle ~90 °(20.0 μs), pulse repetition time 1 s, spectral width 25000 Hz and scan accumulation number 400 - 20000 for enhancement in the S/N ratio. The chemical shifts were reported with respect to 0.1 mol dm^{-3} boric acid solution as an external reference. A 10 mm I.D. NMR sample tube made of PTFE (poly(tetrafluoroethylene)) was employed.

The proton NMR spectra were recorded as described in **CHAPTER 2**.

^{27}Al NMR spectra were recorded at 104.169 MHz. The NMR parameters were typical flip angle ~70 °(20.0 μs), pulse repetition

time 0.658 s, spectral width 25000 Hz and scan accumulation number 200. The chemical shifts were reported with respect to 0.1 mol dm^{-3} aluminium nitrate solution containing 0.1 mol dm^{-3} nitric acid as an external reference. A 10 mm I.D. NMR sample tube was employed.

The sample tube was not rotated during NMR measurements. NMR spectra for an ion-exchanger phase were obtained as described in **CHAPTER 2.**

Determination of volume and ionic concentrations for an anion-exchanger phase

Since highly-charged cations such as aluminium ion are almost entirely excluded from the anion-exchanger, the ^{27}Al NMR spectrum of the anion-exchanger bed containing an aluminium nitrate solution (pH 1.0) should be ascribed to that of the interstitial solution. Thus, the volume fraction of the interstitial solution for the anion-exchanger bed in an NMR sample tube could be obtained from ^{27}Al NMR peak intensities of aluminium ion in the acidic solution with and without the anion-exchanger. The volume fraction of the anion-exchanger skeleton was obtained from ^{1}H NMR peak intensities of H_2O for a sample solution with and without the anion-exchanger.[15,16] The net volume of the anion-exchanger phase was taken as the volume including the skeleton. Thus, the volume of the anion-exchanger phase was calculated from the apparent bed volume and the volume fractions of the skeleton and the resin internal solution by use of eq. 9. The concentrations of the species sorbed into the anion-exchanger phase were expressed in mol dm^{-3}, like an ordinary solution expression. The ionic strength in the ion-exchanger phase was evaluated from the ion-

exchange capacity and expressed like an ordinary solution expression.

RESULTS AND DISCUSSION

Volume and ionic concentrations for the ion-exchanger phase

The net volume of ion-exchanger phase concerned is essential to analyse the complexation equilibria in the ion-exchanger phase. For this purpose, ^{1}H and ^{27}Al NMR spectra for an ion-exchanger bed and for the equilibrium solution only were recorded. Volume fractions for the ion-exchanger bed in an NMR sample tube were determined from these peak intensities (Table 8). The total borate, glycerate and tartrate concentrations in the anion-exchanger phases were 0.0009 - 0.005 mol dm^{-3}, 0.026 - 0.044 mol dm^{-3} and 0.018 - 0.061 mol dm^{-3}, respectively. The ionic strengths obtained for the anion-exchanger phase were $\bar{I}$ = 1.0 for 1-X2, 1.7 for 1-X4 and 2.1 for 1-X8.

Table 8. Volume fractions for an anion-exchange resin bed in an NMR sample tube

Resin	Skeleton (%)	Resin internal solution (%)	Interstitial solution (%)
1-X2	34.3	34.1	31.6
1-X4	41.4	21.4	37.2
1-X8	41.4	25.1	33.5

^{11}B NMR spectra of borate-dihydroxycarboxylate complexes in the anion-exchanger phase

The ^{11}B NMR spectrum for an anion-exchange resin (1-X4) sorbing borate is shown in Fig. 15-[A]. Only one peak appeared at 17.5 ppm and was assigned to $B(OH)_4^-$ in the anion-exchanger phase. The ^{11}B NMR spectra for the anion-exchange resins sorbing borate-glycerate and borate-tartrate are also shown in Fig. 15-[B] and [C]. A new peak appeared at 12.4 - 13.0 ppm besides free borate peak for each spectrum and was assigned to the 1:1 borate-glycerate or borate-tartrate complex. The ^{11}B chemical shift values of these borate species were in good agreement with those for an aqueous solution.[21,22]

Stability constants of borate-dihydroxycarboxylate complexes in the anion-exchange resin phase

For the purpose of comparing the complexibilities in an anion-exchange resin phase and in an aqueous solution, the stability constants of the 1:1 borate-glycerate and borate-tartrate complexes in both phases were evaluated from ^{11}B NMR signal intensities. All stability constant values obtained are given in Table 9.

Complexation equilibria in the resin phase should be complicated by various factors. It was considered that the behaviour of the anion-anion complexation in the anion-exchange resin phase was revealed from a competition between complexation enhancing effect (low water activity and high internal pressure) and lowering effect (low dielectric constant and low ionic mobility). The main reason for lower complexibility in the anion-exchanger phase would be due to repulsive forces between borate and dihydroxycarboxylate ions strengthened by a low dielectric

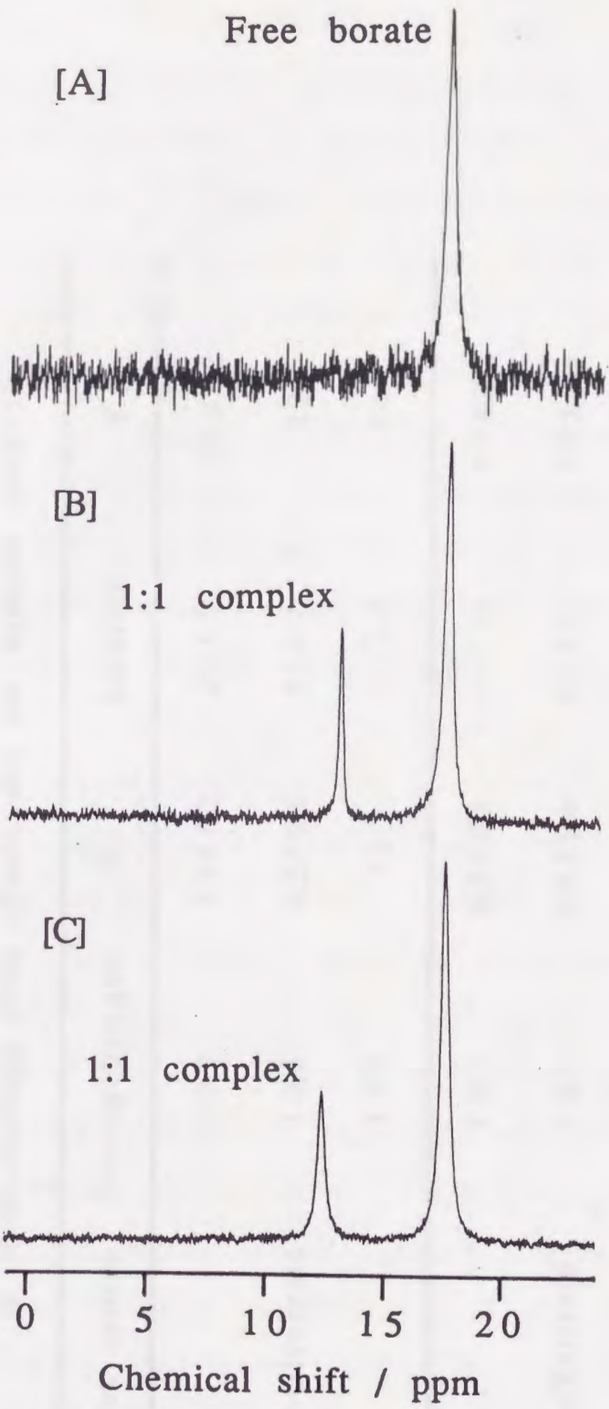

Fig. 15. ^{11}B NMR spectra for borate-dihydroxycarboxylate complex systems in the anion-exchange resin (1-X4) phase;
[A] borate, [B] borate-glycerate and [C] borate-tartrate complex systems.

Table 9. Stability constants of 1:1 borate-dihydroxycarboxylate complexes in anion-exchange resin phases and the aqueous solutions

Complex system	Ion-exchanger	$\overline{K}_1$	Solution	K_1
Borate-Glycerate	1-X2	5.3 ± 0.2	$I = 1.0$	7.9 ± 0.2
	1-X4	6.2 ± 0.1	$I = 1.7$	12
	1-X8	12	$I = 2.1$	14
Borate-Tartrate	1-X2	6.7 ± 0.5	$I = 1.0$	5.6 ± 0.2
	1-X4	6.9 ± 0.6	$I = 1.7$	7.8 ± 0.6
	1-X8	15 ± 1	$I = 2.1$	11

constant. The higher the degree of cross-linking, the lower the dielectric constant, so that the stability constant for the resin phase becomes smaller compared to that for the ordinary aqueous solution. There were, however, little difference between stability constants for the resin phase and the aqueous solution (Table 9), in spite of the lower dielectric constant in the resin phase. This behaviour should be caused by the difference in magnitude between the two competitive effects mentioned above. When the reaction (17) or (18) occurs in the anion-exchange resin, water molecules may readily be liberated due to the low water activity and most of them may be excluded from the resin phase. When water molecules are transferred to the external solution phase from the highly-pressured anion-exchange resin phase, the energy $\pi\Delta V$ is released, as disccused in **CHAPTER 1**. The higher the degree of cross-linking, the lower the water activity and the higher the internal pressure (larger $\pi\Delta V$). Thus, the complexibility in the 1-X8 resin should become higher compared to the 1-X4 resin, despite the larger repulsive force in the 1-X8 resin phase due to lower dielectric constant. If the difference in the complexibilities of 1-X4 and 1-X8 resins is attributed to only the internal pressure, the difference in pressure is calculated to be $\pi = 44 - 52$ atm. In practice, such estimation of the internal pressure is difficult, because of the lower dielectric constant and lower water activity in the 1-X8 resin phase compared to those in the 1-X4 resin phase.

As discussed in this chapter, the complexation equilibria between anionic species in the anion-exchange resin phase were different in various points from those in the aqueous solution and complicated by the competition among various complexation enhancing and lowering effects.

CHAPTER 4. ^{31}P AND ^{13}C NMR SPECTROSCOPIC STUDIES ON PROTONATION EQUILIBRIA OF OXOANIONS IN CROSS-LINKED DEXTRAN GELS

INTRODUCTION

Sephadex gel has been used for chromatographic separation of compounds.[29-31] The Sephadex gel internal phase can be regarded as a heterogeneous polysaccharide solution. The chemical structure of dextran cross-linked by epichlorohydrin is similar to that of cellulose, glycogen or starch which is contained in living matters. The knowledge on complexation in such gel internal solution must be important for understanding chemical reactions in biological media.[13]

In the previous chapters, complexation equilibria for various types of complex systems in ion-exchanger phases investigated by direct spectroscopic methods, were described. It was found that the ion-exchanger rendered complexation enhancing and lowering effects due to characteristic properties such as low dielectric constant, high internal pressure, low water activity, low ionic mobility and spatial restriction.

In the past few years, several authors utilized ^{31}P or ^{13}C NMR to measure an intracelluar pH.[32-38] The method relies on the fact that the chemical shift values of many oxoanions are strongly dependent on pH. However, they overlooked the fact that protonation constants and characteristic chemical shift values in the cell must be different from those in the aqueous solution. Their

assumption may lead to a false conclusion in an equilibrium analysis. In order to clarify the behaviour for protonation of oxoanions in the cell, this chapter will treat protonation equilibria of phosphinate, phosphite and acetate anions in biological model media, such as Sephadex gels.

EXPERIMENTAL

Chemicals

The ^{13}C enriched sodium acetate ($CH_3{}^{13}COONa$) was obtained from Cambridge Isotope Laboratories. All other chemicals were of commercially available reagent grade and used without purification. Uncharged polysaccharide gels of different cross-linking degrees, Sephadex G-10, G-15 and G-25 (Pharmacia, Uppsala, Sweden) were used.

Samples for NMR titration

The solution containing sodium phosphinate, sodium phosphite or sodium acetate was adjusted to required pH and prepared at ionic strength 0.05, 0.1, 0.2 or 0.3 using sodium chloride and hydrochloric acid. An appropriate amount of Sephadex gel (e.g. 1.2 g for Sephadex G-10, 1.0 g for G-15 and 0.7 g for G-25) was equilibrated with 20 cm^3 of the solution. pH measurements were carried out with a combination glass electrode (Horiba 6066-10C) connected with a Horiba pH meter M-13 before and after NMR measurements at 22.5 ± 1 °C. The pH values were converted into $[H^+]$ by using calibration curves of pH vs $[H^+]$ plots or

using activity coefficient values of hydrogen ion reported by Kielland.[39]

NMR measurements

The NMR spectra were recorded on a JEOL JNM-GX 400 spectrometer at probe temperature of 22.5(±1) °C.

The ^{31}P NMR spectra were recorded as described in **CHAPTER 2.**

^{13}C NMR spectra were recorded at 100.533 MHz. The NMR parameters were typical flip angle 45 °(11.5 μs), pulse repetition time 1.5 s, spectral width 22000 Hz and scan accumulation number 500 - 2000. The chemical shifts were reported with respect to sodium 2,2-dimethyl-2-silapentane-5-sulfonate (DSS) as an external reference.

^{17}O NMR spectra were recorded at 54.210 MHz. The NMR parameters were typical flip angle ~80 °(20.0 μs), pulse repetition time 0.38 s, spectral width 43000 Hz and scan accumulation number 1000 - 3500. The chemical shifts were reported with respect to H_2O as an external reference.

NMR spectra for a gel phase were recorded in the same way as those for an ion-exchanger phase (see **CHAPTER 2**).

Determination of volume and hydrogen ion concentrations for a gel phase

In previous chapters, volume fractions for a cation-exchange resin bed in an NMR sample tube were determined from ^{1}H NMR signal intensities.[15,16] In the present study, the volume fraction of the interstitial solution for a Sephadex gel bed in an NMR sample tube was obtained from ^{31}P NMR peak intensities of phosphorus

oxoanion in a sample solution with and without the gel. The volume fraction of the gel skeleton was obtained from ^{17}O NMR peak intensities of H_2O for a sample solution with and without the gel. The net volume of the gel phase was taken as the volume excluding the gel skeleton. Thus, the volume of the gel phase was calculated from the apparent bed volume and the volume fraction of the gel internal solution.

The Sephadex gel was packed into a column and equilibrated with a hydrochloric acid solution whose ionic strength was maintained to 0.05, 0.1, 0.2 or 0.3 using sodium chloride. Then the hydrogen ions in the gel bed were eluted with water and the effluent was titrated with a 0.1 mol dm^{-3} NaOH standard solution. The contribution of the hydrogen ion from the interstitial solution to the titrated value was removed by using the hydrogen ion concentration in the external solution, the apparent bed volume and the volume fraction of the interstitial solution. The hydrogen ion concentration in the gel phase was calculated from the net titrated value for the gel phase and the volume of the gel phase. The concentration was expressed in mol dm^{-3}, like an ordinary solution expression.

RESULTS AND DISCUSSION

Chemical shift trend for oxoanions upon protonation

The ^{31}P signal of phosphinate gave a lowfield shift upon protonation (Fig. 16). Water molecules bound to the phosphinate anion subtract electrons on the phosphorus atom through two oxygen atoms. A cationic hydroxonium ion bound to the anion

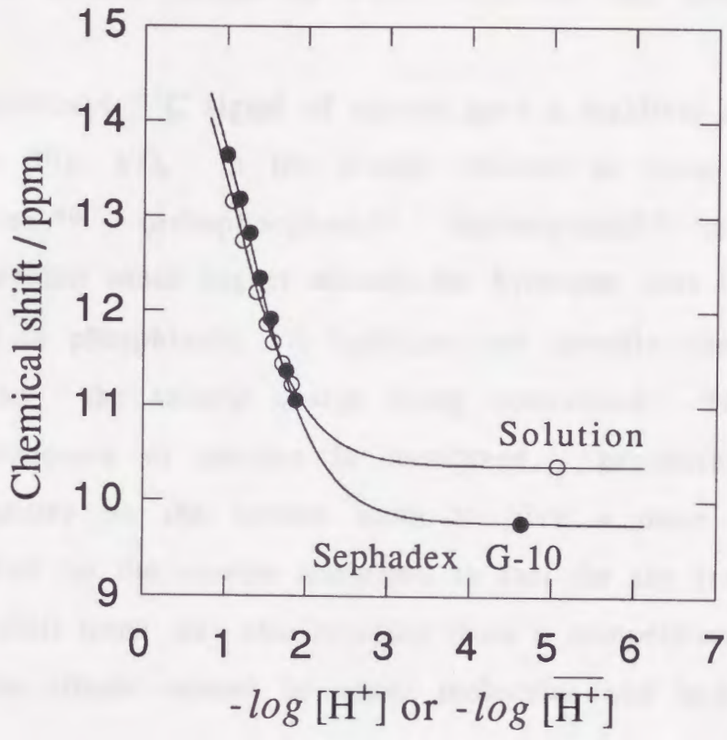

Fig.16. pH titration curves for phosphinate in the Sephadex G-10 phase and the aqueous solution at $I = 0.1$ determined by ^{31}P NMR method.

should subtract electrons on the phosphorus atom more strongly than the water molecule, causing a lowering in electron density on the phosphorus atom to give a more lowfield chemical shift for the protonated phosphinate compared to that for the free anion. In this way, the chemical shift trend was revealed from a difference between two effects caused by water molecules and hydroxonium ions.

The carboxyl ^{13}C signal of acetate gave a highfield shift upon protonation (Fig. 17), in the similar manner as those of other carboxylates,[40] orthophosphate,[41] diphosphate,[41] etc. These oxoanions exhibit much higher affinity for hydrogen ions (high pK_a) compared to phosphinate. A hydrogen ion strongly binds to the acetate anion, the anionic charge being neutralized. Thus, the hydrated structure of acetate is weakened, producing higher electron density on the carbon atom to give a more highfield chemical shift for the species compared to that for the free acetate ion. This shift trend was also revealed from a competition between two opposite effects caused by water molecules and hydroxonium ions.

The NMR signals of other low pK_a oxoanions, such as *cyclo*-triphosphate and trichloroacetate,[42] gave a small magnitude of highfield shift upon protonation due to the difference in magnitude between the two competitive effects mentioned above.

In the same way, the direction of the shift for the phosphite was also interpreted in terms of the two competitive effects. The ^{31}P signal of the species gave highfield shift upon the first protonation and lowfield shift upon the second protonation (Fig. 18). As the phosphite anion is bound strongly by one hydrogen ion (high pK_a), the shift trend at the first protonation should be

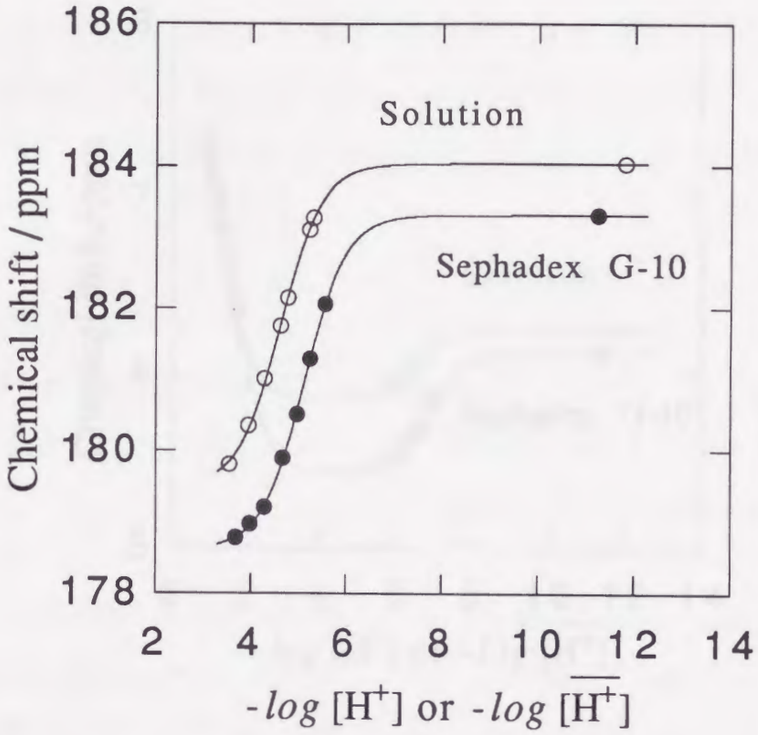

Fig. 17. pH titration curves for acetate in the Sephadex G-10 phase and the aqueous solution at $I = 0.1$ determined by ^{13}C NMR method.

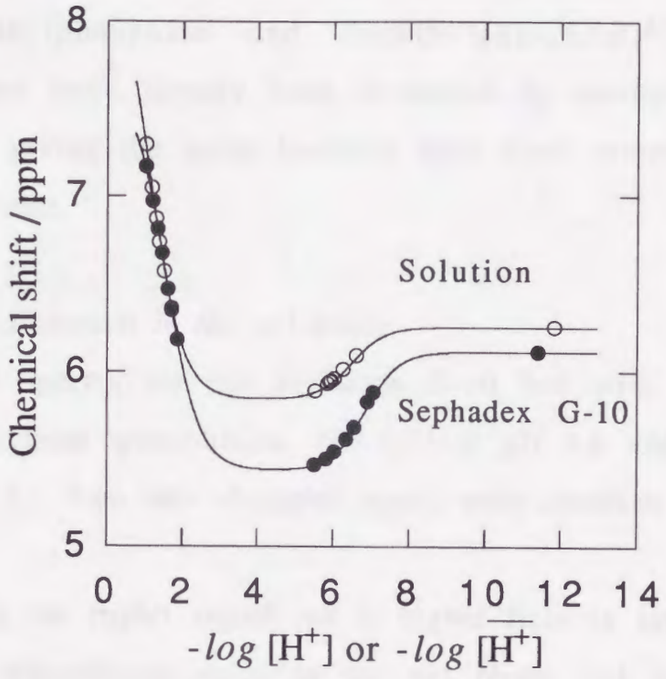

Fig. 18. pH titration curves for phosphite in the Sephadex G-10 phase and the aqueous solution at $I = 0.1$ determined by ^{31}P NMR method.

similar to that for the acetate. On the other hand, the monoprotonated phosphite is bound rather weakly by the next hydrogen ion (low pK_a), the shift trend at the second protonation should be similar to that for the phosphinate.

This interpretation may be applied to general oxoanions, including methylphosphate and dimethylphosphate,[43] whose hydration spheres have already been destroyed by methyl groups, so each signal giving the same lowfield shift upon protonation as that of phosphinate.

NMR spectra of oxoanion in the gel phase

^{31}P NMR spectra for the Sephadex G-10 bed with solutions containing a sodium phosphinate ($I = 0.1$) at pH 4.6 and 1.1 are shown in Fig. 19. Two sets of triplet signal were observed for both spectra.

At pH 4.6 the triplet signal (a) at higher field is assigned to the dissociated phosphinate anion in the gel phase and the triplet signal (b) at lower field to that in the interstitial solution. The hydration state of the anion in the gel phase is different from that in the external solution and the exchange rate of the chemical species between two phases is sufficiently slow. The water activity in the gel phase should be reduced by the presence of organic gel components compared to that in the ordinary aqueous solution. Thus, the phosphinate anion in the gel phase may be somewhat dehydrated compared to that in the aqueous solution, so the ^{31}P NMR chemical shift for the gel phase should be of higher field than that for the aqueous solution as discussed in the previous section.

The ^{31}P resonance of phosphinate showed a lowfield shift upon protonation for both the gel phase and the aqueous solution

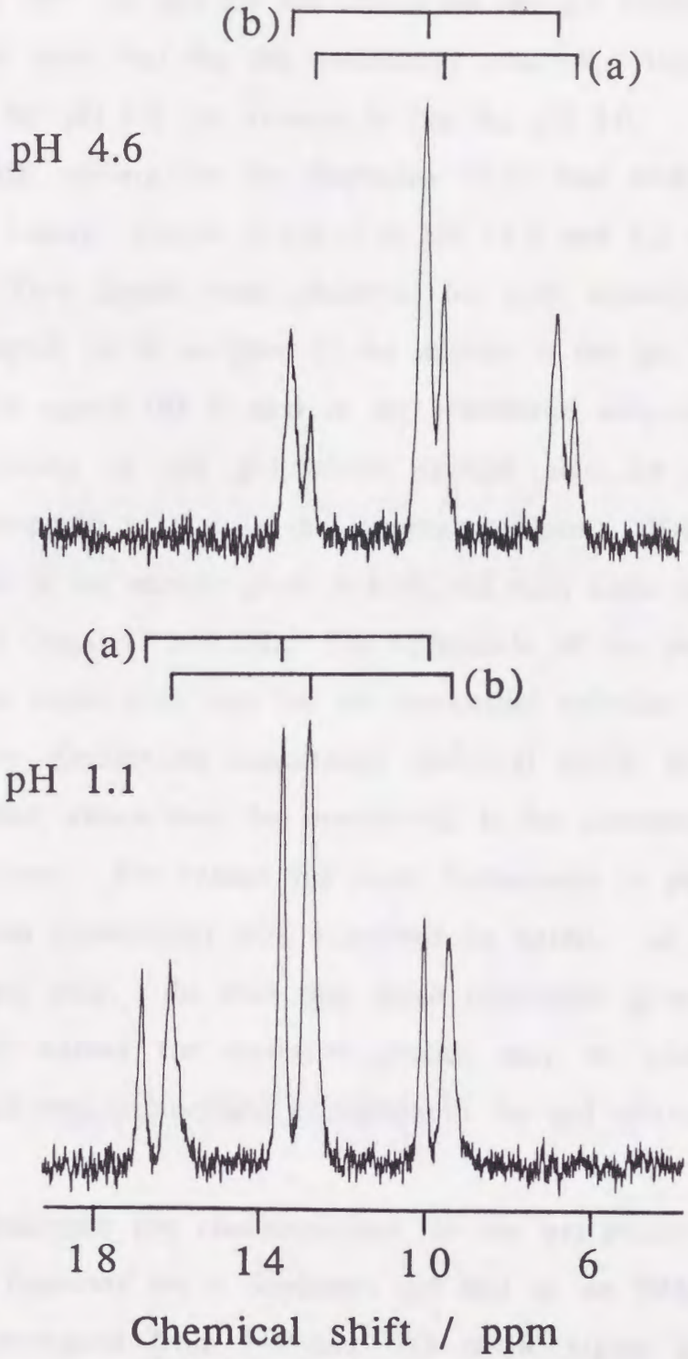

Fig. 19. ^{31}P NMR spectra for the Sephadex G-10 bed with $NaPH_2O_2$ (0.008 mol dm^{-3}) solutions (I = 0.1) at pH 4.6 and 1.1;
(a) Sephadex G-10 phase and (b) interstitial solution.

(Figs. 16 and 19). At pH 1.1 the signal for the gel phase appeared at lower field than that for the interstitial solution, that is, the signals' order for pH 1.1 was reverse to that for pH 4.6.

^{13}C NMR spectra for the Sephadex G-10 bed with solutions containing a sodium acetate ($I = 0.1$) at pH 11.2 and 3.6 are shown in Fig. 20. Two signals were observed for both conditions. The higher field signal (a) is assigned to the acetate in the gel phase and the lower field signal (b) to that in the interstitial solution. Thus, the acetate anion in the gel phase should also be somewhat dehydrated compared to that in the external solution. The carboxyl ^{13}C resonance of the acetate gives a highfield shift upon protonation in both phases (Figs. 17 and 20). The magnitude of the shift for the gel phase was larger than that for the interstitial solution.

All these phenomena concerning chemical shifts in the two phases described above may be considered to be common through general oxoanions. The reason for these behaviours in phosphinate or acetate upon protonation was examined in detail, as discussed below. In any case, the fact that these oxoanions give different chemical shift values for different phases may be conveniently utilized in analysing protonation equilibria in the gel phase.

Volume and hydrogen ion concentrations for the gel phase

Volume fractions for a Sephadex gel bed in an NMR sample tube were determined from ^{31}P and ^{17}O NMR signal intensities (spectra were not shown). The values obtained are shown in Table 10. The net volume of the gel phase was calculated from the volume fraction of the gel internal solution and the apparent bed volume. The concentration of hydrogen ion in the gel phase was determined by a column experiment (see EXPERIMENTAL). The

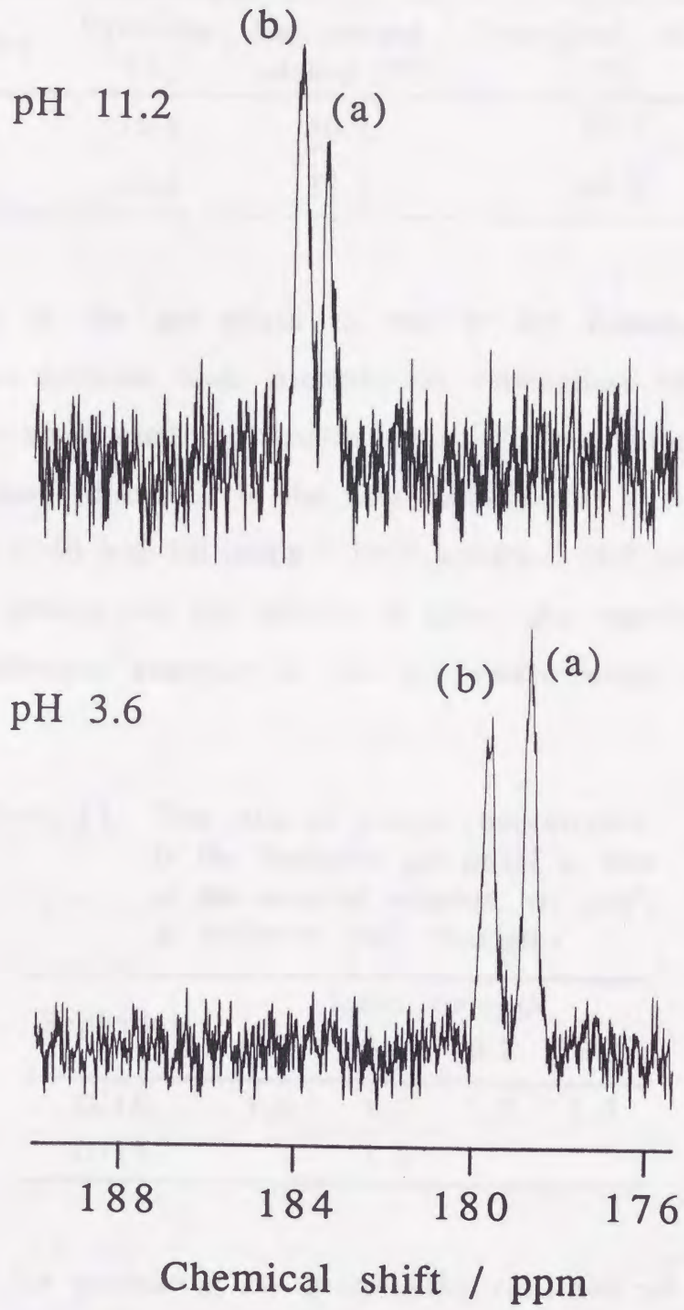

Fig. 20. ^{13}C NMR spectra for the Sephadex G-10 bed with CH_3COONa (0.008 mol dm^{-3}) solutions (I = 0.1) at pH 11.2 and 3.6;
(a) Sephadex G-10 phase and (b) interstitial solution.

Table 10. Volume fractions for a Sephadex gel bed in an NMR sample tube

Sephadex	Skeleton (%)	Gel internal solution (%)	Interstitial solution (%)
G-10	35.6	30.7	33.7
G-15	30.5	32.5	37.0

concentration in the gel phase to that in the external solution ($[\overline{H^+}]/[H^+]$) at different ionic strengths are summarised in Table 11. These values were used for determination of protonation constants in the gel phase (discussed in the next section). It was found that the Sephadex G-10 had 5.6 μeq g^{-1} ionic groups, such concentration of the ionic groups was not enough to cause any significant errors for an equilibrium analysis in the gel phase under conditions studied.

Table 11. The ratio of proton concentration in the Sephadex gel phase to that in the external solution, $[\overline{H^+}]/[H^+]$ at different ionic strengths

Sephadex	Ionic strength			
	0.05	0.1	0.2	0.3
G-10	1.0	1.1	1.2	1.2
G-15		1.1		

NMR method for evaluating the protonation constants of oxoanions in the gel phase

When protonation equilibria of an oxoanion (L) exist in a gel phase, a single time-averaged NMR peak appears and its chemical shift should be given by

$$\bar{\delta}_{obs} = \frac{\bar{\delta}_0[\bar{L}] + \sum_{n=1}^{N} \bar{\delta}_n[\overline{H_nL}]}{[\bar{L}] + \sum_{n=1}^{N} [\overline{H_nL}]} = \frac{\bar{\delta}_0 + \sum_{n=1}^{N} \bar{\delta}_n[\overline{H^+}]^n \prod_{i=1}^{n} \bar{K}_i}{1 + \sum_{n=1}^{N} [\overline{H^+}]^n \prod_{i=1}^{n} \bar{K}_i}; \quad (20)$$

where the upper bar refers to the gel phase, δ_{obs} is the observed chemical shift, δ_0 and δ_n are the chemical shifts of the free and the n-th protonated species, and K_i is the protonation constant for the i-th species. In this equation, $[\overline{H^+}]$ was obtained experimentally for H^+-$PH_2O_2^-$ system (Table 11), but not for H^+-PHO_3^{2-} and H^+-CH_3OO^- systems. The hydrogen ion concentration $[\overline{H^+}]$ was not also obtained for Sephadex G-25, because the volume fractions of the gel phase had not been determined. Thus, $[\overline{H^+}] = [H^+]$ was assumed for these systems, but this assumption could not cause any significant errors, because of $[\overline{H^+}]/[H^+] \approx 1$ for H^+-$PH_2O_2^-$ system (Table 11). Using eq. (20), protonation constants ($\bar{K}_i$) and characteristic chemical shift values ($\bar{\delta}_n$) associated with protonation in Sephadex gels were determined by least-squares fitting to the observed chemical shift values.

Protonation constants and characteristic chemical shift values of oxoanions in a biological model medium

In order to compare protonation equilibria in a gel phase and in an ordinary aqueous solution, the protonation constants of phosphinate, phosphite and acetate anions for Sephadex gels of different cross-linking degrees were evaluated. The least-squares analyses using eq. (20) are shown in Figs. 16, 17 and 18. For comparison, the analyses for aqueous solutions are also shown in the figures. All protonation constants obtained are given in Tables 12 and 13.

Table 12. Protonation constants for the H^+-$PH_2O_2^-$ system in the Sephadex gel phase and the aqueous solution at different ionic strengths

Medium	Ionic strength			
	0.05	0.1	0.2	0.3
Sephadex G-10	23	19	16	14
G-15		17		
G-25		12		
Solution	12	12	11	11

Table 13. Protonation constants of various oxoanions in the Sephadex G-10 phase and the aqueous solution at $I = 0.1$

Medium	H^+-PHO_3^{2-}	H^+-$HPHO_3^-$	H^+-CH_3COO^-
Sephadex G-10	7.2×10^6	37	1.3×10^5
Solution	3.0×10^6	13	4.0×10^4

As can be seen from the tables, the protonation constants for the gel phases are considerably larger than that for the corresponding aqueous solution in all cases. The constant for the gel phase increased with an increase in cross-linking degree.

A protonation of oxoanion in an aqueous medium (including the gel phase) can be divided into hypothetical three steps,

$$\begin{array}{ccc} H^+aq + L^{n-}aq & \xrightarrow{\Delta G} & HL^{(n-1)-}aq \\ \Delta G_1 \downarrow -aq & & \Delta G_3 \uparrow +aq \\ H^+ + L^{n-} & \xrightarrow{\Delta G_2} & HL^{(n-1)-} . \end{array} \qquad (21)$$

Of course, the total free energy change ΔG is the sum of the free energy for each step.

$$\Delta G = \Delta G_1 + \Delta G_2 + \Delta G_3 . \qquad (22)$$

The main reason for the larger protonation constant for the Sephadex gel may be a lowering of water activity for the gel phase compared to the aqueous solution, that is, a lowering of hydration for the species in the gel phase due to the presence of organic skeleton. Thus, the dehydration term ΔG_1 for the gel phase is smaller than that for the aqueous solution. Although the rehydration term ΔG_3 for the gel phase is larger than that for the aqueous solution, its contribution to the total free energy is considerably small compared with ΔG_1, because the degree of hydration for $HA^{(n-1)-}$ in the aqueous medium is much lower than that for the unprotonated species. The ΔG_2 for the protonation in the gaseous state is independent of the water activity. As a whole, ΔG for the gel phase becomes smaller compared to that for the aqueous solution. The higher the degree of cross-linking, the lower the water activity, thus the protonation is more favourable.

Although the protonation constant for the aqueous solution was nearly constant in the range studied, irrespective of the ionic strength, the constant for the Sephadex gel phase increased with a decrease in the ionic strength. The protonation equilibria in the gel phase should be sensitive to the ionic strength due to a low dielectric constant and low degree of hydration for the species, in the same way as those in mixed solvents.[44,45]

Characteristic chemical shift values of oxoanions in the gel phase and in the aqueous solution were also determined by the least-squares analyses (Table 14). The values for the gel phase were always larger than those for the aqueous solution. This indicates that the species in the gel phase should be somewhat dehydrated compared to the species in the aqueous solution.

Several authors utilized NMR chemical shift values of metabolites to measure an intracelluar pH.[32-38] They used the following equation to obtain pH in a cell in terms of the chemical shift of the metabolite as monoprotonated acid,

$$\mathrm{pH} = \log K_1 + log\ \frac{\delta_{obs} - \delta_1}{\delta_0 - \delta_{obs}}. \qquad (23)$$

In the analysis, they employed the same protonation constants and characteristic chemical shift values for metabolites in the cell as those in the ordinary solution without any confirmation. However, these values for the cell should be different from those for the aqueous solution. In fact, it was found that protonation constants and characteristic chemical shift values of oxoanions in the Sephadex gel phase were considerably different from those in the ordinary solution (Tables 12, 13, and 14). The true pH in the gel phase, calculated from the protonation constants and characteristic chemical shift values, is given against the pH obtained by the conventional method (Fig. 21). The correct pH value of an actual

Table 14. Chemical shift values of free and protonated species in the Sephadex gel phase and the aqueous solution at $I = 0.1$

Medium	$PH_2O_2^-$	HPH_2O_2	PHO_3^{2-}	$HPHO_3^-$	H_2PHO_3	CH_3COO^-	CH_3COOH
Sephadex G-10	9.8	15.8	6.1	5.4	7.6	183.3	178.6
Solution	10.4	16.5	6.3	5.8	8.4	184.0	179.5

Chemical shift is expressed in ppm with respect to 85% H_3PO_4 (^{31}P) or DSS (^{13}C).

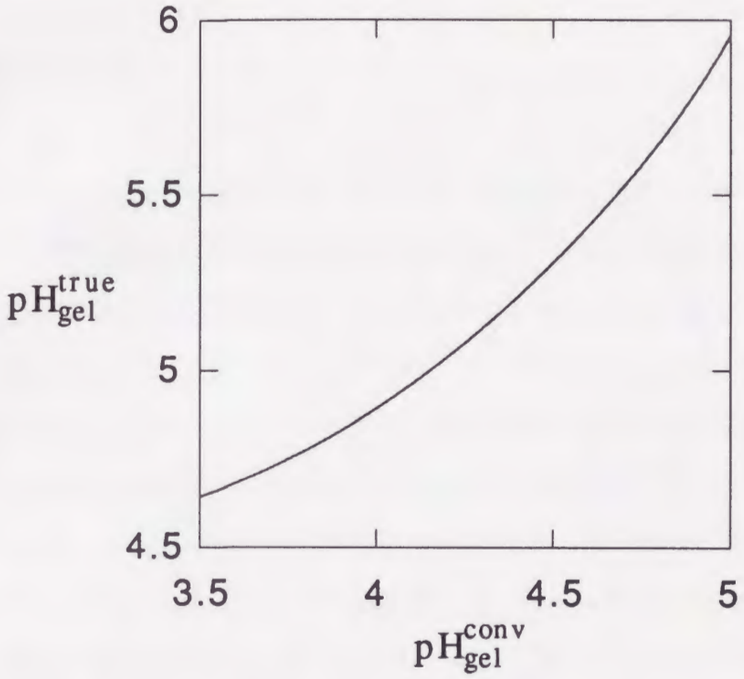

Fig. 21. Comparison between pH values in the Sephadex G-10 phase, determined by using the chemical shift values and the protonation constants of acetate for the gel phase (pH_{gel}^{true}) and the aqueous solution (pH_{gel}^{conv}).

intracelluar solution may be determined only in the treatment described in this section.

CHAPTER 5. ^{27}Al NMR SPECTROSCOPIC STUDIES ON COMPLEXATION EQUILIBRIA OF ALUMINIUM ION IN CROSS-LINKED DEXTRAN GELS

INTRODUCTION

In the previous chapter, NMR spectroscopic studies on the protonation properties of oxoanions in the Sephadex gel phase were presented. It was found that a gel renders protonation enhancing effects.

Interests for the complexation of aluminium ion with various ligands originated from several research fields.[46-48] It is said that aluminium is a suspect playing a role in Alzheimer disease.[49,50] This chapter will treat ^{27}Al NMR spectroscopic studies on the complexation equilibria of aluminium ion with phosphinate, thiocyanate or sulphate anions in biological model media, such as Sephadex gels. Since the ligand exchange rate of the aluminium complex is sufficiently slow relative to the NMR time-scale, NMR signals can be observed independently for different complexes. Nevertheless, the complexation reaches to equilibrium within few minutes at room temperature, and the information on complexation equilibria in the gel phase may be obtained easily by using ^{27}Al NMR spectroscopy.

EXPERIMENTAL

Chemicals

All chemicals were of commercially available reagent grade and used without purification. Uncharged polysaccharide gels of different cross-linking degrees, Sephadex G-10, G-15 and G-25 (Pharmacia, Uppsala, Sweden) were used.

Samples for NMR measurements

A 0.005 mol dm^{-3} aluminium nitrate solution containing sodium phosphinate (pH 1.1 - 1.5), sodium thiocyanate (pH 2.5) or sodium sulphate (pH 2.0), was prepared at ionic strength 0.1, 0.5, or 1.5 using sodium nitrate. The pH values of the solutions were adjusted to pH 1.1 - 2.5 with a small amount of nitric acid solution in order to avoid the formation of the aluminium hydroxo complexes. An appropriate amount of Sephadex gel (e.g. 1.2 g for Sephadex G-10, 1.0 g for G-15 and 0.7 g for G-25) was equilibrated with 20 cm^3 of the solution in a stoppered test tube at room temperature for 3 - 6 h.

NMR measurements

The NMR spectra were recorded on a JEOL JNM-GX 400 spectrometer at probe temperature of 22.5(±1) °C.

The ^{31}P and ^{27}Al NMR spectra were recorded as described in **CHAPTER 2** or **3**.

NMR spectra for the gel phase were recorded in the same way as those for an ion-exchanger phase (see **CHAPTER 2**).

Determination of volume and ionic concentrations for a gel phase

In the previous chapter, the volume fractions for a Sephadex gel bed in an NMR sample tube were determined by using ^{31}P and ^{17}O NMR signal intensities (Table 10). The net volume of the gel phase was taken as the volume excluding the gel skeleton. Thus, the volume of the gel phase was calculated from the apparent bed volume and the volume fraction of the gel internal solution.

Phosphinate anion concentration in the Sephadex gel phase was determined from the concentration in the equilibrated solution, ^{31}P NMR signal intensities and the volume fractions for the gel bed. Corrections were made for a protonation of the anion in the gel phase by using the protonation constants reported in the previous chapter.

The concentrations of thiocyanate and sulphate anions in the Sephadex gel phase were determined by column operations. The gel beads were packed into a column and equilibrated with 0.5 mol dm^{-3} sodium thiocyanate or sodium sulphate solution. Then, the ligand anions in the gel bed were eluted with water and the amount in the effluent was determined. The contribution of ligand anions from the interstitial solution to the obtained value was removed by using the ligand anion concentration in the external solution, the apparent bed volume and the volume fraction of the interstitial solution. The ligand anion concentration in the gel phase was calculated from the net amount for the gel phase and the volume of the gel phase. The concentration was expressed in mol dm^{-3}, like an ordinary solution expression.

RESULTS AND DISCUSSION

Ligand anion concentration in the gel phase

The ^{31}P NMR spectrum for the Sephadex G-10 bed with a solution ($I = 0.1$, pH 1.4) containing 0.005 mol dm^{-3} aluminium nitrate and 0.008 mol dm^{-3} sodium phosphinate is shown in Fig. 22. Three sets of triplet signal were observed. The lowest field triplet signal was assigned to the free and protonated phosphinate in the gel phase, the second lowest triplet signal to the species in the interstitial solution and the highest triplet signal to the $AlPH_2O_2^{2+}$ complexes in both the gel phase and the interstitial solution. The signals of the complex could not be observed separately for each phase. Thus, the concentration of free phosphinate anion in the gel phase could be determined from the concentration in the equilibrated solution, the volume fractions for the gel bed and the ^{31}P signal intensities of the species for each phase. The corrections were made for a side reaction upon protonation by using the protonation constants. The free phospinate anion concentration obtained was used for determination of the stability constants of the 1:1 aluminium complex in the gel phase.

The concentrations of thiocyanate and sulphate anions in the Sephadex gel phase were determined by column operations (see EXPERIMENTAL).

The ratios of ligand anion concentration in the gel phase to that in the external solution ($[\bar{L}]/[L]$) are summarised in Table 15, where the ratios for the phosphinate anion under no supporting electrolyte added and under a neutral condition are listed. As can be seen from the table, the affinity of these anions for the gel phase increases in the order: $SO_4^{2-} < PH_2O_2^- < SCN^-$. This order is in

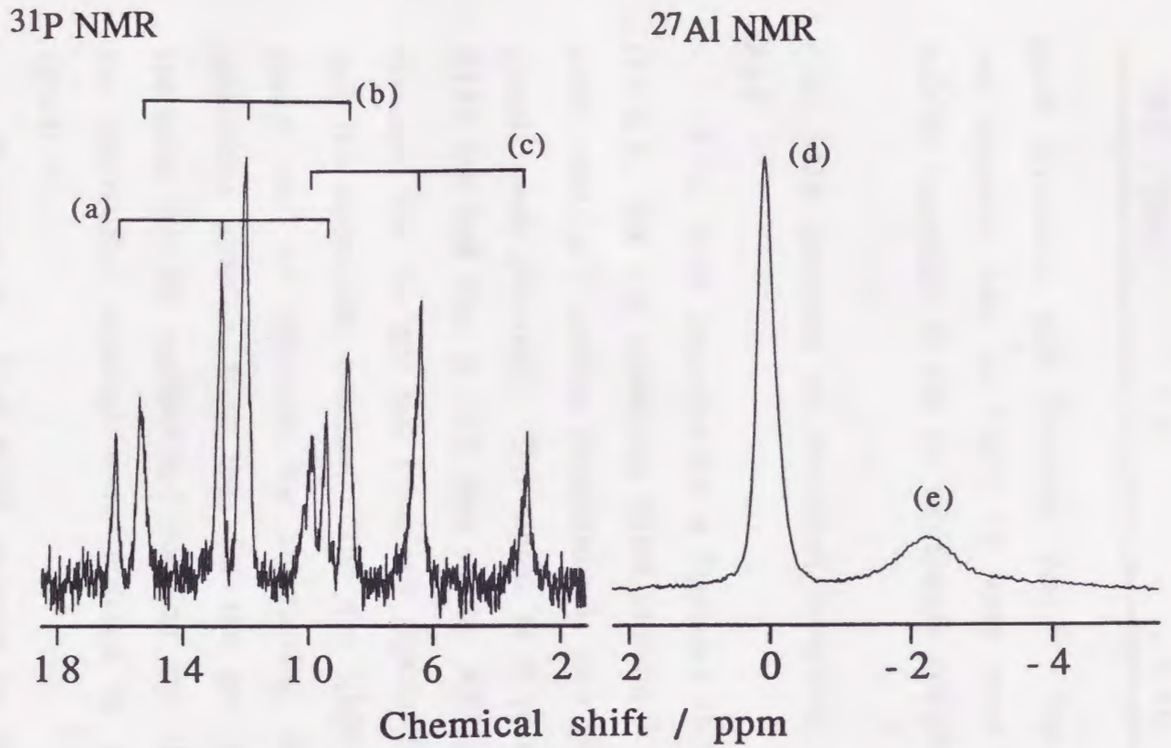

Fig. 22. ^{31}P and ^{27}Al NMR spectra for the Sephadex G-10 bed with a solution ($I = 0.1$, pH 1.4) containing 5×10^{-3} mol dm^{-3} $Al(NO_3)_3$ and 8×10^{-3} mol dm^{-3} $NaPH_2O_2$;

(a) HPH_2O_2 and $PH_2O_2^-$ in the gel phase,

(b) HPH_2O_2 and $PH_2O_2^-$ in the external solution,

(c) $AlPH_2O_2^{2+}$ in the bed,

(d) Al^{3+} and (e) $AlPH_2O_2^{2+}$ in the bed.

Table 15. The ratio of ligand anion concentration in the Sephadex gel phase to that in the external solution

$[\bar{L}]/[L]$	Ionic strength	Sephadex G-10	Sephadex G-15
$[\overline{PH_2O_2^-}]/[PH_2O_2^-]$	0.1	0.68	1.0
$[\overline{SCN^-}]/[SCN^-]$	0.5	2.0	1.8
$[\overline{SO_4^{2-}}]/[SO_4^{2-}]$	1.5	0.45	0.56

good agreement with literature data.[31] The ratios for thiocyanate and sulphate ions in Table 15 were used for determination of stability constants of the 1:1 aluminium complexes in the gel phase.

^{27}Al NMR spectrum of aluminium complexes for the Sephadex gel bed

^{27}Al NMR spectrum for a Sephadex G-10 bed with a solution (I = 0.1, pH 1.4) containing 0.005 mol dm^{-3} aluminium nitrate and 0.008 mol dm^{-3} sodium phosphinate is also shown in Fig. 22. Two signals were observed. The signal at 0 ppm was assigned to the Al^{3+} ion and that at -3.3 ppm to the $AlPH_2O_2^{2+}$ complex. The spectrum for the gel bed contained signals for both the gel phase and the interstitial solution. The net NMR spectrum for the gel phase can be obtained by subtracting the spectrum for the interstitial solution from that for the gel bed. Therefore, the spectrum for the equilibrated solution and the volume fraction of the interstitial solution were utilized to obtain the gel phase spectrum.

Furthermore, ^{27}Al NMR spectrum for the gel bed with a 0.005 mol dm^{-3} aluminium nitrate solution containing 0.5 mol dm^{-3} sodium thiocyanate or sodium phosphinate was recorded (Fig. 23). The siganls for the $AlSCN^{2+}$ (at 4.7 ppm) and $AlSO_4^+$ (at 3.1 ppm)

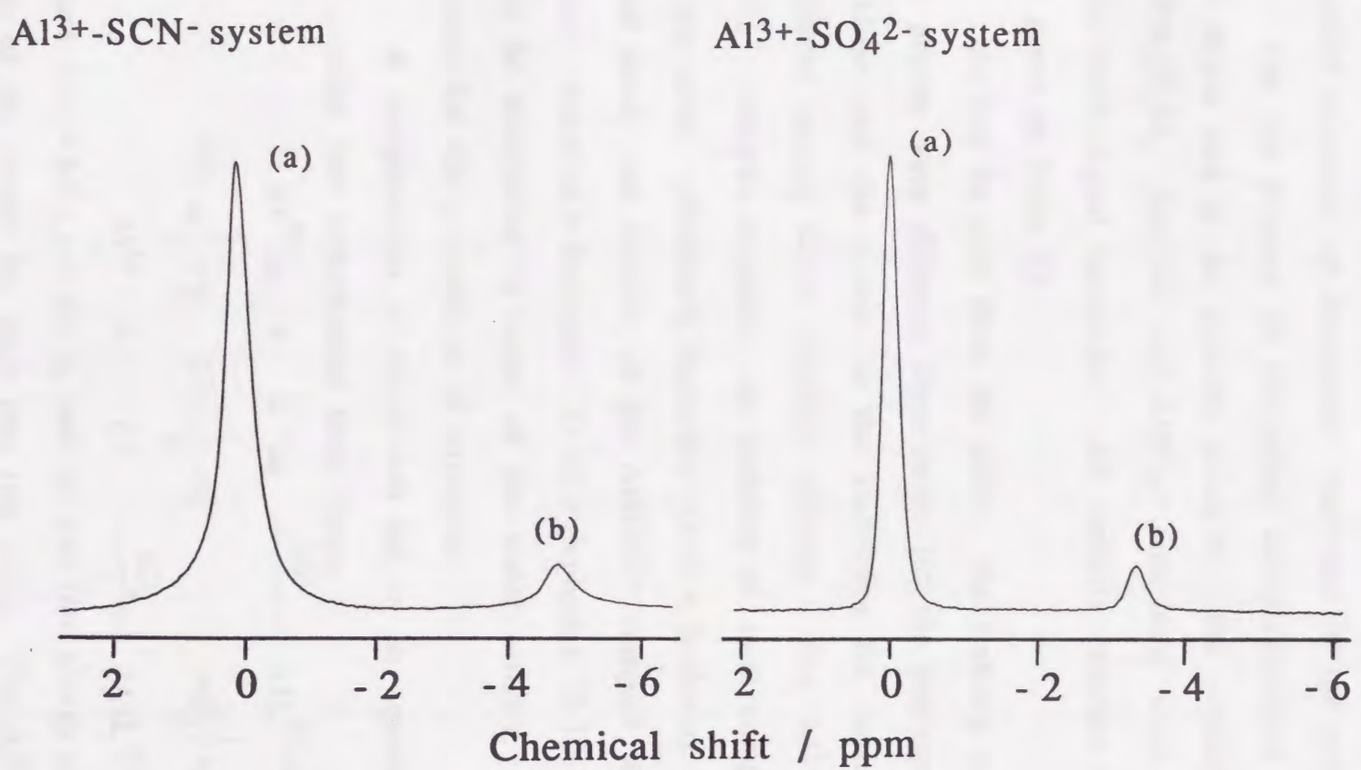

Fig. 23. ^{27}Al NMR spectra of aluminium complexes for the Sephadex G-10 bed; Sephadex gel beds with $5x10^{-3}$ mol dm^{-3} $Al(NO_3)_3$ solution containing 0.5 mol dm^{-3} NaSCN (pH 2.5) or 0.5 mol dm^{-3} Na_2SO_4 (pH 2.0); (a) Al^{3+} and (b) the 1:1 complex in the gel bed.

complexes also appeared for each spectrum besides the free Al^{3+} signal.

Stability constants of aluminium complexes in the gel phase

For the purpose of comparing complexibilities in a Sephadex gel phase and in an aqueous solution, the stability constants of $AlPH_2O_2^{2+}$, $AlSCN^{2+}$ and $AlSO_4^{+}$ complexes were evaluated from ^{27}Al NMR signal intensities. All stability constant values obtained are given in Table 16.

As can be seen from the table, the stability constants for the gel phases were different from those for the corresponding aqueous solution and the orders in the stabilities for each medium were different among these complex systems. For Al^{3+}-$PH_2O_2^{-}$ and -SO_4^{2-} complex systems, the stability of these complexes increased in the order: solution < Sephadex G-15 < Sephadex G-10. On the other hand, the stability of the $AlSCN^{2+}$ complex decreased in the order: solution > Sephadex G-15 > Sephadex G-10. These trends may be interpreted in terms of the water activity, in the similar process for the protonation of oxoanion.

A complexation of aluminium ion in an aqueous medium can be divided into hypothetical three steps,

$$\begin{array}{ccccc} Al^{3+}aq & + & L^{n-}aq & \xrightarrow{\Delta G} & AlL^{(3-n)+}aq \\ \Delta G_{1,Al}\downarrow -aq & & \Delta G_{1,L}\downarrow -aq & & \Delta G_3\uparrow +aq \\ Al^{3+} & + & L^{n-} & \xrightarrow{\Delta G_2} & AlL^{(3-n)+} \end{array} , \qquad (24)$$

where $\Delta G_1 = \Delta G_{1,Al} + \Delta G_{1,L}$ and the toal free energy change ΔG is the sum of the energy for each step (eq. (22)). For Al^{3+}-$PH_2O_2^{-}$ and -SO_4^{2-} complex systems, the dehydration term $\Delta G_{1,L}$ for the gel phase is smaller than that for the aqueous solution, because of low

Table 16. Stability constants of aluminium complexes in the Sephadex gel phase and the aqueous solution

Complex system	Ionic strength	Sephadex G-10	Sephadex G-15	Solution
Al^{3+}-$PH_2O_2^-$	0.1	(2.8 ± 0.1)x10	(2.2 ± 0.1)x10	(1.7 ± 0.1)x10
Al^{3+}-SCN^-	0.5	0.08 ± 0.01	0.19 ± 0.01	0.47 ± 0.04
Al^{3+}-SO_4^{2-}	1.5	0.63 ± 0.08	0.44 ± 0.02	0.22 ± 0.01

water activity in the gel phase. Thus, the stability constants of these complexes for the gel phase became larger compared to those for the aqueous solution. The higher the degree of cross-linking, the lower the water activity, thus the complexation is more favourable. In the case of Al^{3+}-SCN^- complex system, $\Delta G_{1,L}$ for the gel phase is comparable to that for the aqueous solution due to the low degree of hydration for the thiocyanate ion. The absolute value of the rehydration term ΔG_3 for the gel phase may be larger than that of $\Delta G_{1,L}$, because of the low water activity in the gel phase and the higher degree of hydration for the $AlSCN^{2+}$ complex compared to the free anion. Thus, the stability constant of the complex in the gel phase became smaller compared to that in the aqueous solution. The higher the degree of cross-linking, the more unfavourable the complexation in the gel phase, due to the lower water activity.

As mentioned above, the NMR method is a very powerful one in the analysis of the complexation equilibria in the cross-linked polysaccharide gel. The complexibilities of aluminium ion in the gel phase and the aqueous solution were different each other and the order of stabilities for aluminium complexes in each phase depends upon the hydration ability of the ligand.

CONCLUSIONS

Although a cross-linked polymer gel is a solid in appearance, it can be regarded as a concentrated heterogeneous polymer solution and as a model of a biological medium. The complexation reactions and the states of chemical species in a gel phase can be considerably different in various points from those in an ordinary aqueous solution. In the present study, direct spectroscopic methods (electronic and NMR spectroscopies) were successfully applied to the analysis of complexation equilibria for the solid phase. It is found that the gel has complexation enhancing and lowering effects due to some factors such as low dielectric constant, high internal pressure, low water activity, low ionic mobility and spatial restriction.

CHAPTER 1. The direct equilibrium analyses for inorganic cobalt(II) complexes in cation- and anion-exchanger solid phases were successfully made by the visible absorption spectroscopy. It was found that stability constants of the one-to-one cobalt(II)-isothiocyanate complex in the cation-exchanger phases with different cross-linking degrees are in all cases intrinsically higher than those in the solutions under the corresponding condition. This result should be ascribed to low dielectric constant and high internal pressure which are characteristic to the ion-exchanger phase, in comparison with the solution phase.

CHAPTER 2. The analysis of the complexation in a cadmium-phosphinate system in the cation-exchanger phase was satisfactorily performed by ^{31}P NMR method. The ^{31}P NMR signal of phosphinate anion shifted to opposite directions in cation- or anion-exchangers.

Stability constants of the $CdPH_2O_2^+$ complex in the cation-exchanger phase were considerably smaller compared with those in the corresponding solutions. This result can be attributed to low ionic mobility and spatial restriction in the ion-exchanger phase as compared with the ordinary solution. From the fact that the chemical shift value of the $CdPH_2O_2^+$ complex for the cation-exchanger phase is larger than that in the solution, it is assumed that the chelate form of the complex is predominant in cation-exchanger phases.

CHAPTER 3. The complexation by oxygen atom linkage between borate and dihydroxycarboxylate in the anion-exchange resin phase was investigated by ^{11}B NMR spectroscopy. The complexation equilibria of borate-glycerate and borate-tartrate in the anion-exchange resin phase were different in various points from those in the aqueous solution and complicated by the competition between complexation enhancing and lowering effects which were characteristic to the anion-exchange resin.

CHAPTER 4. The protonation equilibria of phosphinate, phosphite and acetate anions in uncharged polysaccharide gels were analysed by ^{31}P and ^{13}C NMR methods. These oxoanions gave different chemical shift values in the gel phase and the external solution. The chemical shift for the gel phase is a value of higher field compared to that for the external solution. The direction of chemical shift of an oxoanion upon protonation was correlated to its pK_a. The protonation constants of oxoanions in the gel phase were larger than those in the corresponding solutions without exception. These results should be interpreted in terms of a lower water activity in the gel phase than in the ordinary aqueous solution.

CHAPTER 5. The complexation equilibria of aluminium ion with phosphinate, thiocyanate and sulphate anions in the uncharged polysaccharide gel phase were investigated by using ^{27}Al NMR spectroscopy. The interpretation for the protonation of oxoanion in the gel phase was extended to understand the complexation. The stability constants of $AlPH_2O_2^{2+}$ and $AlSO_4^+$ complexes for the gel phase were larger and that of $AlSCN^{2+}$ complex for the same phase was smaller than those for each corresponding solution. These phenomena must be interpreted in terms of a low water activity in the gel phase and a different hydration ability of the anions.

Above all, we established quantitative approaches to the complexation equilibria in the cross-linked polymer solution like ion-exchangers by means of spectroscopic methods such as electronic and NMR spectroscopies. We can state that the same kinds of spectroscopic methods would be applied to the equilibrium analyses for biological media and the models. Effects influencing the complexation in the cross-linked polymer solution would also affect general biochemical reactions in biological media, so that our results obtained in the present study should give important information for general biochemical reactions.

REFFERENCES

1. R. M. Smith and A. E. Martell (Eds), *Critical Stability Constants, Iorganic Complexes*, Vol. 4. Plenum Press, New York (1976).
2. E. Högfeldt (Ed.), *Stability Constants of Metal-Ion Complexes*, Part A: Inorganic ligands. Pergamon Press, Oxford (1982).
3. L. G. Sillén and A. E. Martell (Eds), *Stability Constants of Metal-Ion Complexes*, Special Publication No. 17. London (1964).
4. L. G. Sillén and A. E. Martell (Eds), *Stability Constants of Metal-Ion Complexes*, Special Publication No. 25. London (1971).
5. H. Waki, S. Takahashi and S. Ohashi, *J. Inorg. Nucl. Chem.* 1973, **35**, 1259.
6. K. Yoshimura, H. Waki and S. Ohashi, *J. Inorg. Nucl. Chem.* 1977, **39**, 1697.
7. H. Waki, S. Noda and M. Yamashita, *Reactive Polymers* 1988, **7**, 227.
8. H. Waki and G. Kura, *Fresenius Z. Anal. Chem.* 1985, **320**, 268.
9. J. Schubert, *J. Phys. Chem.* 1948, **52**, 340.
10. J. Schubert and A. Lindenbaum, *J. Am. Chem. Soc.* 1952, **74**, 3529.
11. W. C. Bauman and J. Eichhorn, *J. Am. Chem. Soc.* 1947, **69**, 2832.
12. Y. Marcus and A. S. Kertes, *Ion Exchange and Solvent Extraction of Metal Complexes*, Wiley-Interscience, London (1964).
13. R. Damadian, *Ann. N. Y. Acad. Sci.* 1973, **204**, 261.
14. I. Hosokawa and F. Ohshima, *Water Res.* 1973, **7**, 283.

15. J. P. de Villiers and J. R. Parrish, *J. Polymer Sci., Part A* 1964, 1331.
16. R. W. Creekmore and C. N. Reilley, *Anal. Chem.* 1970, **61**, 570.
17. H. Waki and Y. Miyazaki, Proceedings of Ion Exchange Advances '92, Elsevier Science Publishers Ltd, 1992, p191.
18. Q. Feng and H. Waki, *Polyhedron* 1990, **9**, 1555.
19. Q. Feng and H. Waki, *Polyhedron* 1991, **7**, 659.
20. J. Boeseken, *Adv. Carbohydr. Chem.* 1949, **4**, 189.
21. M. V. Duin, J. A. Peters, A. P. G. Kieboom and H. V. Bekkum, *Tetrahedron* 1984, **40**, 2901.
22. M. V. Duin, J. A. Peters, A. P. G. Kieboom and H. V. Bekkum, *Tetrahedron* 1985, **41**, 3411.
23. N. Ingri, *Acta Chem. Scand.* 1962, **16**, 439.
24. F. A. Cotton and G. Wilkinson, *Advanced Inorganic Chemistry*, 5th Ed., p169.
25. J. X. Khym and L. P. Zill, *J. Am. Chem. Soc.* 1952, **74**, 2090.
26. R. Sargent and W. Rieman, *Anal. Chim. Acta* 1957, **16**, 144.
27. A. S. Schwok, Y. Feitelson and J. Rabani, *J. Phys. Chem.* 1981, **85**, 2222.
28. Y. Kurimura, M. Nagashima, K. Takato, E. Tsuchida, M. Kaneko and A. Yamada, *J. Phys. Chem.* 1982, **86**, 2432.
29 V. D. Gregorio and M. Sinibaldi, *J. Chromatogr.* 1976, **129**, 407.
30 T. Deguchi, A. Hisanaga and H. Nagai, *J. Chromatogr.* 1977, **133**, 173.
31 K. Yoshimura and T. Tarutani, *J. Chromatogr.* 1982, **237**, 89.
32 R. B. Moon and J. H. Richards, *J. Biol. Chem.* 1973, **248**, 7276.
33 S. J. W. Busby, D. G. Gadian, G. K. Radda, R. E. Richards and P. J. Seeley, *Biochem. J.* 1978, **170**, 103.

34 J. K. M. Roberts and O. Jardetzky, *Biochim. Biophys. Acta* 1981, **639**, 53.

35 J. K. M. Roberts, N. W. Jardetzky and O. Jardetzky, *Biochemistry* 1981, **20**, 5389.

36 Y. Seo, M. Murakami, H. Watari, Y. Imai, K. Yoshizaki, H. Nishikawa and T. Morimoto, *J. Biochem.* 1983, **94**, 729.

37 P. Lundberg, E. Harmsen, C. Ho and H. J. Vogel, *Anal. Biochem.* 1990, **191**, 193.

38 P. M. L. Robitaille, P. A. Robitaille, G. G. Brown Jr. and G. G. Brown, *J. Magn. Reson.* 1991, **92**, 73.

39 J. Kielland, *J. Am. Chem. Soc.* 1937, **59**, 1675.

40 R. E. London, *J. Magn. Reson.* 1980, **38**, 173.

41 M. M. Crutchfield, C. F. Irani and G. C. Roth, *Inorg. Chem.* 1962, **1**, 813.

42 K. Tsuruta, Y. Miyazaki and H. Waki, unpublished data.

43 K. Moedritzer, *Inorg. Chem.* 1967, **6**, 936.

44 J. S. Firtz and H. Waki, *J. Inorg. Nucl. Chem.* 1964, **24**, 865.

45 H. Waki and J. S. Firtz, *J. Inorg. Nucl. Chem.* 1966, **28**, 577.

46 C. T. Driscoll, J. P. Baker, J. J. Bisogni and C. L. Schofield, *Nature* 1980, **284**, 161.

47 S. C. Tam and R. J. P. Williams, *J. Inorg. Biochem.*, 1986, **26**, 35.

48 W. Hölderich, M. Hesse and F. Näumann, *Angew. Chem.*, 1988, **100**, 232.

49 D. R. Crapper S. S. Krishnan and A. J. Dalton, *Science* 1973, **180**, 511.

50 D. P. Perl, *Environ. Health Perspect.*, 1985, **63**, 149.

ACKNOWLEDGMENTS

The author expresses his deep gratitude to Professor Hirohiko Waki for his unfailing encouragement, kind advice and guidance throughout this graduate work.

The author also wishes to thank Associate Professor Kazuhisa Yoshimura and the entire staffs at the Laboratory of Analytical Chemistry in Kyushu University for their valuable suggestion and continuous encouragement.

The author thanks Professor Tsutomu Katsuki and Associate Professor Yoshio Ito for their help in the acquisition of the NMR data.

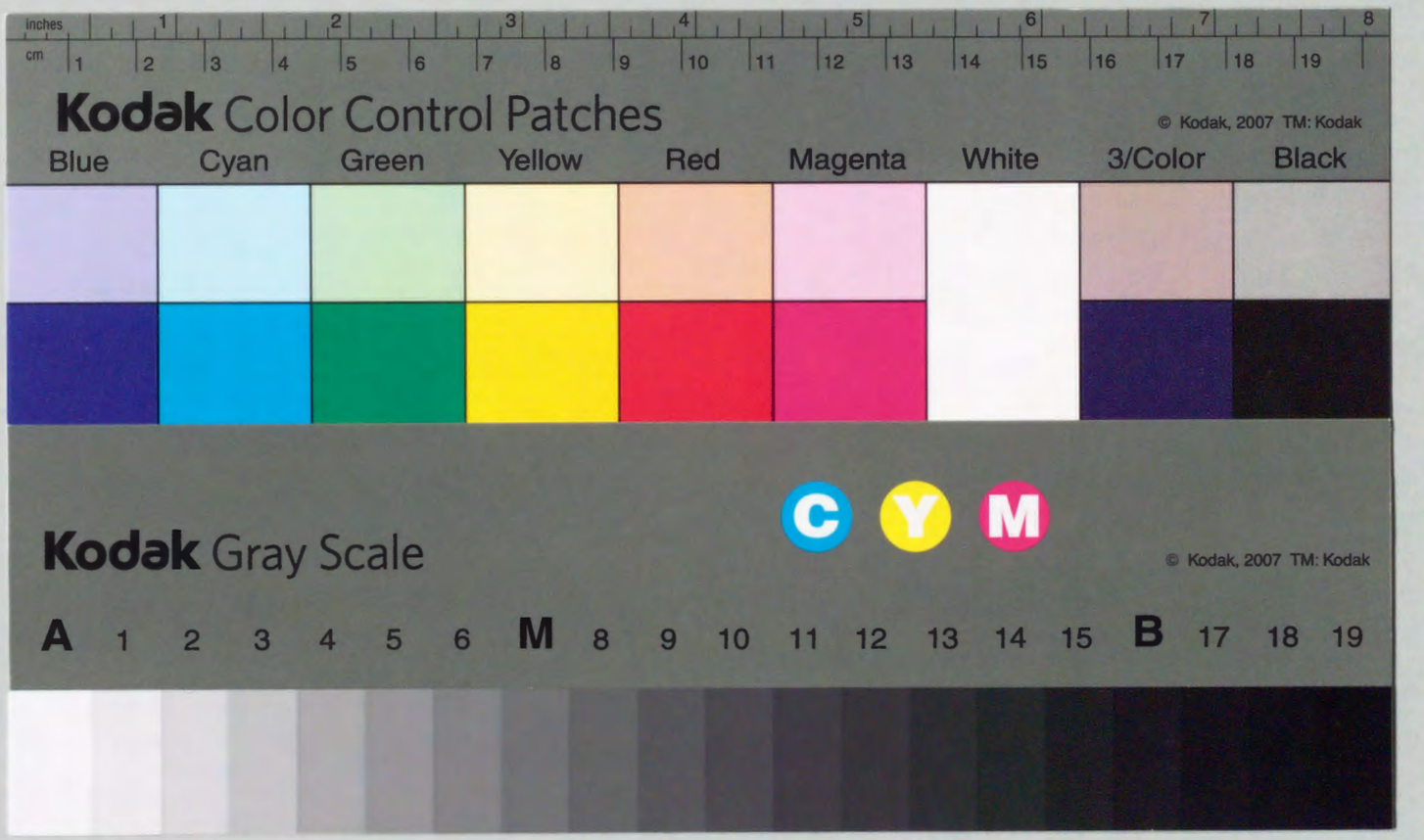
inches
cm
Kodak Color Control Patches
© Kodak, 2007 TM: Kodak
Blue
Cyan
Green
Yellow
Red
Magenta
White
3/Color
Black
Kodak Gray Scale
C
Y
M
© Kodak, 2007 TM: Kodak
A 1 2 3 4 5 6 M 8 9 10 11 12 13 14 15 B 17 18 19